NATIONAL TECHNICAL UNIVERSITY OF ATHENS
SCHOOL OF NAVAL ARCHITECTURE AND MARINE ENGINEERING
DEPARTMENT OF SHIP DESIGN & MARITIME TRANSPORT

DIPLOMA THESIS

Numerical validation of the "critical wave groups" method for the probabilistic assessment of ship stability in irregular beam seas

GEORGIOS PAPAGEORGIOU

SUPERVISOR: PROFESSOR KONSTANTINOS J. SPYROU

ATHENS
FEBRUARY 2017

Acknowledgements

The current thesis represents the final chapter of my studies at the National Technical University of Athens. First and foremost, I would like to express my deepest appreciation to my supervisor, Professor Konstantinos J. Spyrou, who sparked my passion for ship dynamics through his teaching and gave me the opportunity to get involved in such an interesting thesis project. It is an honour for me to have worked closely with him and I am thankful for his valuable support throughout the duration of the project.

Furthermore, I would like to express my sincere gratitude to Mr. Panayiotis Anastopoulos, PhD candidate, whose assistance towards the completion of the project was invaluable. I am indebted to him for his precious guidance and countless hours he spent assisting me. Without him, the completion of the thesis would not be possible.

Last but not least, I am thankful to my parents for their endless support during my studies.

Summary

This thesis deals with the numerical validation of the "critical wave groups" method that was developed by Themelis & Spyrou (2007) for the probabilistic assessment of ship stability. The method approximates the probability of ship instability by the probability of encountering any wave group that could have provoked the instability. In the original formulation of the method, ship dynamic stability was tested against regular waveforms. In this work, the focus is set on the study of ship roll motions in irregular beam seas and a reformulation of the "critical wave groups" method is attempted by employing realistic wave group excitations. The latter derive from the method of Anastopoulos et al. (2016) and represent the "most expected" wave groups of a sea state. The probability of exceeding a number of different heeling angles is computed and the results are compared to those obtained when assuming regular wave groups, as in the original methodology. Comparisons with the distribution of roll angles calculated by direct Monte Carlo simulations of ship motion are also included. The results indicate that consideration of irregular wave groups leads to more accurate results for a range of small to medium heeling angles. Possible ways to improve the method are proposed and its practicality for the assessment of ship stability is discussed.

Περίληψη

Η παρούσα διπλωματική εργασία πραγματεύεται την αριθμητική επαλήθευση της μεθόδου των "critical wave groups" η οποία αναπτύχθηκε από τους Themelis & Spyrou (2007) για την πιθανοθεωρητική αξιολόγηση της ευστάθειας του πλοίου. Η μέθοδος υποθέτει ότι η πιθανότητα αστάθειας ισούται με την πιθανότητα το πλοίο να συναντήσει οποιαδήποτε κυματική ομάδα ("wave group") που είναι ικανή να προκαλέσει την εν λόγω αστάθεια. Σε πρώτο στάδιο, η μέθοδος υλοποιήθηκε χρησιμοποιώντας κανονικές (αρμονικές) κυματικές ομάδες. Η παρούσα εργασία επικεντρώνεται στη μελέτη της απόκρισης του πλοίου σε διατοιχισμό υπό την επίδραση ανεμογενών πλευρικών κυματισμών και για το λόγο αυτό επιχειρείται η βελτίωση της μεθόδου των "critical wave groups", χρησιμοποιώντας ρεαλιστικότερες κυματομορφές. Οι τελευταίες προκύπτουν από την εργασία των Anastopoulos et. al. (2016) που υπολογίζει τις "πιο αναμενόμενες" κυματικές ομάδες για δεδομένη κατάσταση θάλασσας. Έτσι, γίνεται εκτίμηση της πιθανότητας υπέρβασης ενός εύρους γωνιών διατοιχισμού και τα αποτελέσματα συγκρίνονται με αυτά που προκύπτουν θεωρώντας κανονικές κυματομορφές, όπως στην αρχική μεθοδολογία. Τα αποτελέσματα συγκρίνονται επίσης με την κατανομή των γωνιών διατοιχισμού που παράγονται με απευθείας Monte-Carlo προσομοιώσεις της κίνησης του πλοίου. Από τις συγκρίσεις αυτές φαίνεται ότι η χρήση ρεαλιστικότερων κυματομορφών βελτιώνει την ακρίβεια της μεθόδου των "critical wave groups". Τέλος, προτείνονται πιθανοί τρόποι για την περαιτέρω βελτίωση της μεθόδου.

Table of Contents

List of Figures

List of Tables

1. Introduction

Providing a vessel with sufficient stability in realistic seaways is still a challenging task in naval architecture due to the complexity of the phenomena related to capsizing in a random environment. Capsizing is a sudden event, often completed in a short time period that poses a significant threat to both the safety of human life at sea and the environment. Thus, it is a matter of major concern to the International Maritime Organization (IMO). The developments in the design and operation of commercial ships over the last decades as well as the advances in the understanding of the mechanisms that might lead a ship to capsize were the motivation behind IMO's new intact stability criteria, commonly known as the "2nd Generation Intact Stability Criteria", which are currently under development. IMO acknowledged the fact that new criteria should be based on the physics of the specific phenomena leading to stability failure rather than on simplistic statistical models of failures. At the same time, it was agreed that the new criteria should be related to the probability of stability failure.

Roll dynamic stability is often evaluated under certain simplifications regarding the nature of the excitation that is modelled in a deterministic context. These models, although providing an insight into the mechanisms of capsizing, are inadequate for a probabilistic analysis of roll motions in wind generated seas. On the other hand, capsize is a rare phenomenon and thus, performing "brute-force" numerical simulations for calculating the probability of extreme events becomes a computationally expensive procedure that does not lead essentially to accurate results. Therefore, one could argue that it is more efficient to develop alternative methodologies, focusing only on those time periods when ship is susceptible to capsizing.

An interesting phenomenon, often observed in wind generated seas, is the encounter of sequences of high waves having nearly equal periods, commonly known as "wave groups" (e.g., Ochi, 1998) (Figure 1.). Besides, it is widely known among fishermen and seamen that "a large wave rarely comes alone". Knowledge of the characteristics of wave groups is of importance since they can provoke resonant response due to the small variation of the periods of the individual waves as well as extreme ship motions when the waves are considerably high. The phenomenon was first described by Longuet-Higgins and Steward (1962) and ever since many researchers have worked on developing methodologies for predicting wave group statistics.

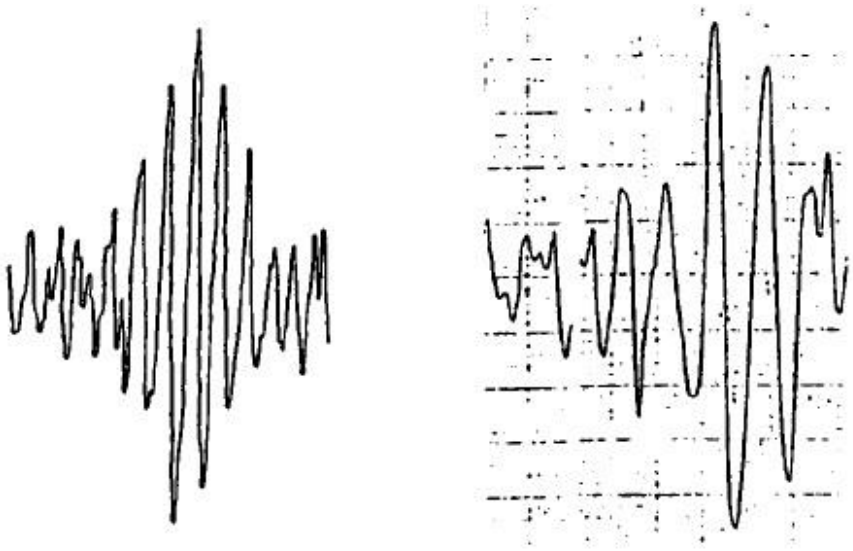

Figure 1.1 Examples of wave groups observed at sea (Ochi, 1998)

Efforts towards deploying the concept of wave groups for ship stability assessment were made only recently. A significant contribution to the topic is the "critical wave groups" method proposed by Themelis and Spyrou (2007), which approximates the probability of any type of ship instability (e.g., parametric roll, beam seas resonance, pure-loss of stability) by the probability of encountering any wave group that could have provoked the instability. The method provides a versatile solution to the problem of "rarity", described in the above, by solving separately two sub-problems, the "deterministic" and the "probabilistic". In the deterministic part, ship dynamic stability is tested against regular wave groups. The target is to identify the "critical wave groups" that is, those specific wave groups which; given the period and run length[1], incur loss of stability with the lowest height. In the probabilistic part of the approach, the probability of encountering any wave group that is higher than the determined critical is calculated using spectral methods and assuming that associated height and period sequences are Markov-chains. The method has become popular over the years being a practical tool for the development of the IMO 2nd Generation Intact Stability Criteria.

The objective of this thesis is to evaluate the accuracy of the "critical wave groups" method for calculating the probability of large amplitude ship motions in beam seas. To this end, we address the following assumptions of the originally proposed methodology:

[1] Number of consecutive waves with heights greater than a specified threshold.

1. To allow for a more realistic representation of the wave loads involved in the deterministic part of the approach, we replace regular waveforms by the "most expected" wave groups, given a sea state, which derive from the application of the method developed by Anastopoulos et al. (2016).
2. To eliminate the uncertainty related to the accuracy of the "spectral methods", employed in the probabilistic part of the approach, desirable distributions of wave heights and periods are obtained from direct Monte Carlo simulations of the water surface elevation.

As realized, the first assumption implies a reformulation of the "critical wave groups" method in terms of irregular wave group excitations. Thus, to evaluate if in such case the accuracy of the method is improved, both formulations are tested against Monte Carlo simulations of ship roll motion.

Therefore, this thesis is structured as follows:

Chapter 2 is a literature review on the advances of wave group theory and its implementation for the evaluation of ship stability. In Chapter 3 the method of Anastopoulos et al. (2016) is revisited and an alternative approach regarding the construction process of time-continuous irregular waveforms groups is proposed. In Chapter 4 we present the mathematical model of roll motion that was used for the identification of the critical wave groups. Chapter 5 includes an application of the "critical wave groups" method on a modern containership. The probability of exceeding different heeling angles is calculated using both regular and the realistic wave group excitations and the results are validated by Monte Carlo simulations of ship roll motion. In Chapter 6 the above results are discussed and possible ways for further improving the method and its practicality for ship stability assessment are proposed.

2. Literature review

2.1 Advances in wave group theory

A first model to describe the statistical properties of wave groups was given by Goda (1970) who assumed statistical independence between successive wave heights. Several studies attempted to validate Goda's assumption by elaborating on data obtained by wave field measurements (e.g., Wilson and Baird, 1972; Rye, 1974; Goda, 1976; Dattari et al., 1977). Their conclusion however was that Goda's theory was under-predicting wave group statistics.

Rye (1974) noticed that the dependence between successive wave heights is not negligible and thus, wave heights have a "memory" by which it is more likely that a high wave is followed by another high wave. In other words, the heights of successive waves should be correlated. Rye (1974) was the first to compute the correlation coefficient of successive wave heights based on a record of 5400 individual waves obtained from field measurements in the North Sea.

Arhan and Ezraty (1978) assumed that the joint probability distribution of successive wave heights could be approximated reasonably well by the joint probability distribution of two values of the theoretical envelope of the water surface elevation (see Figure 2.1). Moreover, they computed the correlation coefficient of successive wave heights from a record of 26000 waves observed in the North Sea.

The next step was taken by Kimura (1980) who evaluated the probability of occurrence of wave groups within the context of the theory of Markov processes. Based on the results of Arhan & Ezraty (1978), he adopted the bivariate Rayleigh distribution for the statistical description of consecutive wave heights. Furthermore, he assumed that consecutive periods follow the bivariate Weibull distribution. The associated correlation parameters were calculated from direct Monte Carlo simulations of the wave field.

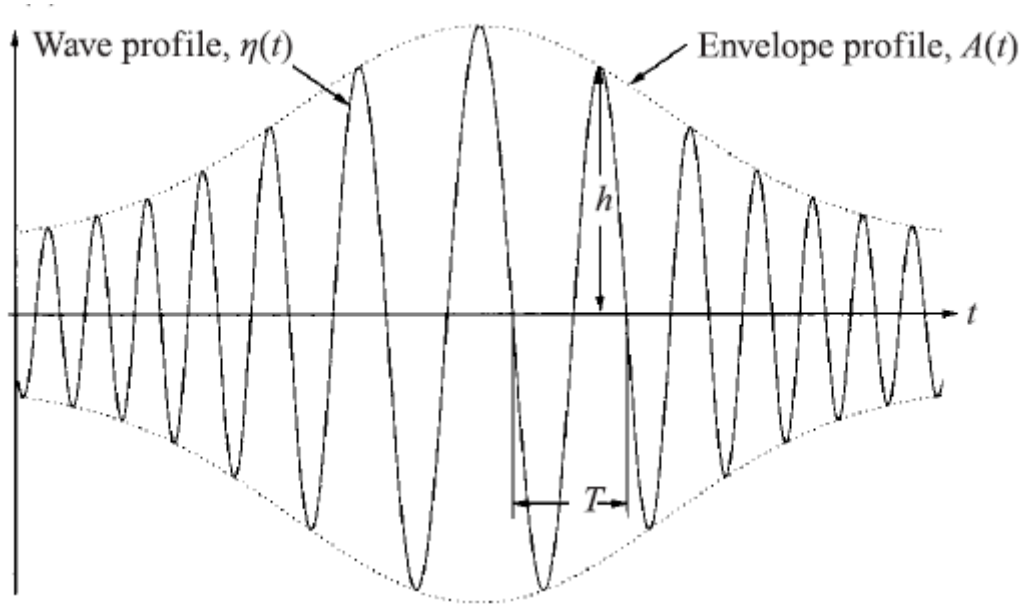

Figure 2.1 Example of envelope process (Stansell et al., 2004)

To alleviate the computational burden of the Monte Carlo approach, Battjes & van Vledder (1984) employed spectral methods. In more detail, they proposed a simple formula for the calculation of the correlation parameter of successive wave heights based on the joint distribution of two points of the theoretical envelope separated by the mean spectral period and assuming that the wave height is twice the local amplitude. Later, van Vledder (1992) derived an alternative formula for the same correlation parameter by elaborating on the joint probability distribution of four values of the envelope process separated by half the mean spectral period; thus, considering that crest and trough heights are not necessarily equal.

Stansell et al. (2002) analyzed wave data collected from a fixed steel jacket oil and gas platform in the northern North Sea. The purpose of the specific study was to validate the Markov assumption when dealing with wave group statistics. Therefore, the mean and standard deviation of the run length was estimated in two different ways: a) by direct counting and b) by assuming that consecutive wave heights follow the bivariate Rayleigh distribution. In the latter case, the correlation parameter was computed either by direct counting or by employing spectral methods (e.g., Battjes & van Vledder, 1984; van Vledder, 1992). The conclusion was that the assumption of the bivariate Rayleigh distribution with correlation parameter derived directly from the analyzed time series compares well to the direct counting approach. On the other hand, the correlation parameter proposed by van Vledder (1992) leads to satisfactory results only in the case of low spectral bandwidths.

Despite that many studies have dealt with the evaluation of the correlation coefficient between successive wave heights, little progress was made, until recently, with respect to the corresponding periods. Anastopoulos et al. (2016) improved the model of Kimura (1980) by proposing an extended Markov-chain model that incorporates the cross-correlations between successive wave heights and periods. To this end, the theory of copula distributions was employed and copula parameters were derived from an efficient computational procedure based on the statistics of the envelope process. The accuracy of the method for the prediction of the "most expected" wave heights and associated periods was tested against Monte Carlo simulations. The results were satisfactory in the case of wave heights, yet conservative for the related periods. Finally, the continuous-time counterparts of the "most expected" height and period sequences were constructed by applying the Karhunen-Loève theorem according to the method described in Sclavounos (2012).

2.2 Implementation of the wave group theory in the evaluation of ship stability

Kim & Troesch (2013) proposed a novel approach for generating realistic wave profiles that lead to extreme parametric roll responses. In order to do so, they deployed the Design Loads Generator (DLG) (Kim et al., 2011) to determine the group of waves that cause extreme metacentric height variations (GM), when the latter is considered a Gaussian random process. Once the wave profiles are known, high fidelity hydrodynamic tools are employed to calculate the distribution of roll angles. To justify Gaussianity in the variation of GM, the authors interpret the results as the lower bound of the "true" extreme roll response. Comparisons with Monte-Carlo simulations indicate that the accuracy of the method is low.

Malara et al. (2014) proposed a method for the calculation of the maximum roll angle of a vessel under the effect of spectrum compatible wave group loads, modelled within the context of the "Quasi-Determinism" theory (Boccotti, 2000). The reliability of the maximum roll angle calculation was investigated in terms of the ratio of the obtained maximum roll angle to the standard deviation of the response derived from direct Monte Carlo simulations. Nonetheless, the results are conservative possibly due to the fact that the theory of "Quasi-Determinism" is asymptotically valid for infinitely high waves (Boccotti, 2000). Another weakness of the method is that the periods of the individual waves of any "Quasi-Deterministic" waveform always vary within a fixed range, making the study of resonant phenomena impossible.

Anastopoulos & Spyrou (2016) conducted a preliminary investigation of the effect of irregular wave group forms on the transient response of a 4800 TEU containership. Their work extends the concept of the "critical wave groups method" of Themelis & Spyrou (2007) by substituting the regular wave trains by the "most expected" wave group profiles, given a sea state, derived from the application of the method described earlier in Anastopoulos et al. (2016). Comparisons between the "Transient Capsize Diagrams"[2] produced for the cases of regular and realistic wave group excitations revealed a wider and shifted instability region, attributed to the variation of the individual periods of the irregular wave groups.

[2] Transient capsize diagrams are plots of wave period against wave steepness ratio associated with critical, from ship dynamics perspective, roll angles (Rainey & Thompson, 1991)

3. Irregular wave groups – method of construction

3.1 Introduction

In this chapter we describe the method developed by Anastopoulos et al. (2016) for the systematic construction of the "most expected" irregular wave groups, given a sea state. The method consists of two parts concerning: a) modelling of discrete-time wave height and period sequences within the context of Markov processes and b) construction of the continuous-time counterparts of derived sequences by applying the Karhunen-Loève theorem. In the first part, the transition mechanisms of the extended Markovian system are given in the form of conditional expectations of successive wave heights and related periods. Closed forms for the transition probabilities are provided in terms of copula distributions. In the second part of the approach, a new method for the continuous-time representation of the "most expected" wave height and related period sequences is developed by employing Fourier series as an alternative to the originally proposed Karhunen-Loève scheme.

Before proceeding into a more detailed mathematical description of wave groups, the following definitions, regarding their structure, are necessary:

- The height of an individual wave H is defined by the maximum vertical excursion of the free surface elevation between two consecutive zero up-crossings.
- The period of an individual wave T is equal to the time difference between two consecutive zero up-crossings.
- The run length j is the number of consecutive waves that exceed a certain threshold H_{cr} (see also Figure 3.1Figure 3.1 Wave group with three consecutive wave heights exceeding a threshold $\boldsymbol{H_{cr}}$.).

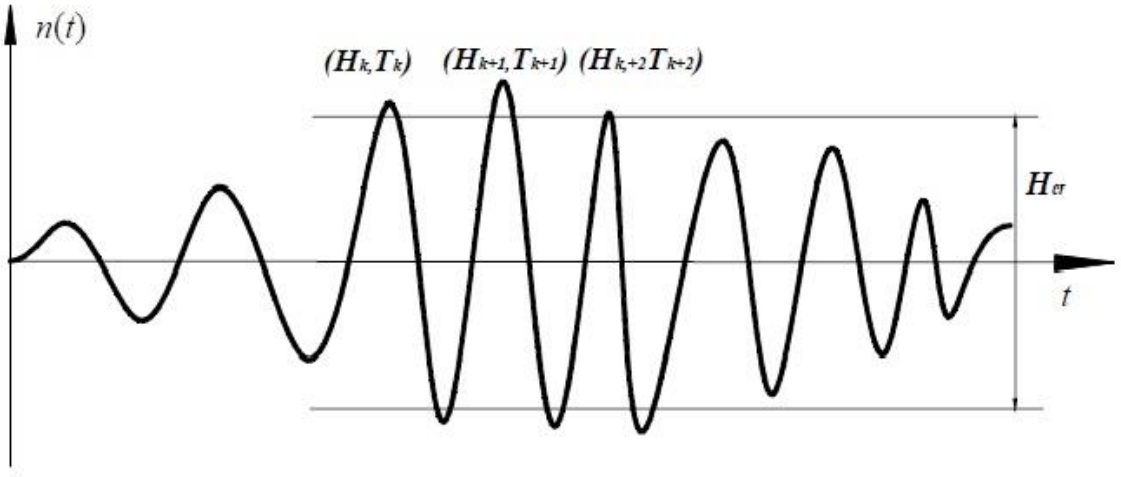

Figure 3.1 Wave group with three consecutive wave heights exceeding a threshold H_{cr}.

3.2 Identification of the "most expected" height and period sequences

3.2.1 Definition of the extended Markov process

A Markov process is a stochastic process X_t for which the future state $x(t_{n+1})$ depends only on the current state $x(t_n)$ and not on the previous states $x(t_1), \ldots\ldots, x(t_{n-1})$ i.e., it has no memory of how the present state was reached. This absence of memory is called "Markovian property". In other words, for the Markovian process X_t and for $t_1 < t_2 < \cdots < t_n$ it holds that:

$$P[X(t_n) \leq x_n | X(t_{n-1}), \ldots\ldots, X(t_1)] = P[X(t_n) \leq x_n | X(t_{n-1})] \qquad (3.1)$$

In this thesis we deal only with Markov chains of discrete time – continuous state and the following notation will be adopted for the state variables: $x(t_i) = x_i, i = 1,2 \ldots$

Equation (3.1) implies that the conditional joint probability density function of n consecutive realizations of X_t is:

$$f_{X_n|X_{n-1},\ldots,X_1}(x_n|x_{n-1}, \ldots, x_1) = f_{X_n|X_{n-1}}(x_n|x_{n-1}) \qquad (3.2)$$

and according to the chain rule:

$$f_{X_1,\dots,X_n}(x_1,\dots,x_n) = f_{X1}(x_1)\cdot\prod_{i=2}^{n} f_{X_i|X_{i-1}}(x_i|x_{i-1}) \tag{3.3}$$

where $f_{X_i|X_{i-1}}(x_i|x_{i-1})$ is the transition probability density of the process. We say that a Markov process is time-homogenous when the latter is the same at every time step i.

Another property of a Markov process is time-reversibility which states that the properties of the process do not change if the time is reversed, that is:

$$f_{X_n|X_{n+1},\dots,X_{n+k}}(x_n|x_{n+1},\dots,x_{n+k}) = f_{X_n|X_{n+1}}(x_n|x_{n+1}) \tag{3.4}$$

In the case of two successive waves, the joint probability density function of their heights H_i and periods T_i derives from equation (3.2):

$$f_{H_i,T_i|H_{i-1},T_{i-1}}(h_i,t_i|h_{i-1},t_{i-1}) = \frac{f_{H_{i-1},T_{i-1},H_i,T_i}(h_{i-1},t_{i-1},h_i,t_i)}{f_{H_{i-1},T_{i-1}}(h_{i-1},t_{i-1})} \tag{3.5}$$

where h_i and t_i are the state variables of the random variables H_t and T_t at time step i, respectively.

Anastopoulos et al. (2016) assumed that the above Markovian processes are cross-correlated and time-homogenous. Thus, the conditional expectations of h_i and t_i at any time step i are determined by the following equations:

$$\overline{h_i} = \int_0^\infty h_i f_{H_i|H_{i-1},T_{i-1}}(h_i|h_{i-1},t_{i-1})dh_i \tag{3.6}$$

$$\overline{t_i} = \int_0^\infty t_i f_{T_i|H_i,H_{i-1},T_{i-1}}(t_i|h_i,h_{i-1},t_{i-1})dt_i \tag{3.7}$$

The most expected sequences of wave heights and related periods can be determined by applying the equations (3.6) and (3.7) iteratively, using the height and period of the highest wave of the group as initial conditions (Anastopoulos et al., 2016). Taking advantage of the time-reversibility property, the most expected heights and periods of the waves preceding the highest can be determined by replacing i with $i-1$ and $i-1$ with i in equations (3.6) and (3.7). Under these terms, the highest wave is always encountered at the middle of a symmetric wave train.

3.2.2 Calculation of the transition probabilities

Below, analytic forms for the transition mechanisms that appear in equations (3.6) and (3.7) are provided in terms of copula probability distributions. The latter are a special case of joint probability distributions that allow studying the degree of dependence among random variables separately from the effects of the marginal distributions. The strength of dependence between the involved variables in a copula expression is controlled by correlation parameters. One can choose from a variety of copulas that are available in the literature when fitting observed data. However, there is no prior knowledge of which copula is most appropriate for a specific application. Thus, several copula models have to be employed so as to conclude which fits better the examined population. The approach becomes more efficient when the statistical qualities of the latter are known (Anastopoulos et al., 2016).

In the following, $F_{X,Y}$ will be the bivariate cumulative distribution function (CDF) of the random variables $X,\ Y$ with marginals F_X, F_Y, respectively. According to Sklar's theorem (1959) the relationship of the above distributions and a copula C is:

$$F_{X,Y}(x,y) = C(F_X(x), F_Y(y)) \tag{3.8}$$

According to the probability integral transform, the marginals F_X and F_Y can be regarded as random variables uniformly distributed over $(0,1)$ thus, C takes the form of a bivariate distribution. In the case of conditional copulas, the theorem is extended as (Patton, 2006):

$$F_{X,Y|W}(x,y|w) = C(F_{X|W}(x|w), F_{Y|W}(y|w)|w) \tag{3.9}$$

As a result of the Bayes theorem, the following equation holds:

$$F_{X|Y,W}(x|y,w) = \frac{F_{X,Y|W}(x,y|w)}{F_{Y|W}(y|w)} \tag{3.10}$$

By applying equation (3.9) on equation (3.10) we obtain:

$$F_{X|Y,W}(x|y,w) = \frac{C(F_{X|W}(x|w), F_{Y|W}(y|w)|w)}{F_{Y|W}(y|w)} \tag{3.11}$$

The transition probability of equation (3.6) is derived by reformulating equation (3.11) in terms of the wave heights and periods of successive waves:

$$F_{H_i|H_{i-1},T_{i-1}}(h_i|h_{i-1},t_{i-1}) = \frac{C(F_{H_i|T_{i-1}}(h_i|t_{i-1}), F_{H_{i-1}|T_{i-1}}(h_{i-1}|t_{i-1})|t_{i-1})}{F_{H_{i-1}|T_{i-1}}(h_{i-1}|t_{i-1})} \tag{3.12}$$

In the same spirit, the transition probability of equation (3.7) becomes:

$$F_{T_i|H_i,H_{i-1},T_{i-1}}(t_i|h_i,h_{i-1},t_{i-1}) =$$

$$\frac{C(F_{T_i|H_{i-1},T_{i-1}}(t_i|h_{i-1},t_{i-1}), F_{H_i|H_{i-1},T_{i-1}}(h_i|h_{i-1},t_{i-1})|h_{i-1},t_{i-1})}{F_{H_i|H_{i-1},T_{i-1}}(h_i|h_{i-1},t_{i-1})} \tag{3.13}$$

and the first term of the numerator of equation (3.13) is:

$$F_{T_i|T_{i-1},H_{i-1}}(t_i|t_{i-1},h_{i-1}) = \frac{C(F_{T_i|H_{i-1}}(t_i|h_{i-1}), F_{T_{i-1}|H_{i-1}}(t_{i-1}|h_{i-1})|h_{i-1})}{F_{T_{i-1}|H_{i-1}}(t_{i-1}|h_{i-1})} \tag{3.14}$$

According to Anastopoulos et al. (2016), a good model for the numerators of equations (3.12) and (3.14) is the bivariate Gaussian copula:

$$C(u,v) = \int_{-\infty}^{\Phi^{-1}(u)} \int_{-\infty}^{\Phi^{-1}(v)} \frac{1}{2\pi\sqrt{1-\rho^2}} e^{-\frac{z(x,y)}{2(1-\rho^2)}} dxdy \tag{3.15}$$

where ρ is the correlation coefficient, Φ^{-1} is the inverse of the univariate standard Normal distribution function:

$$\Phi^{-1}(u) = \sqrt{2} erf^{-1}(2u - 1) \tag{3.16}$$

and

$$z(x, y) = x^2 + y^2 + \rho xy \tag{3.17}$$

The marginal conditional distributions were derived by combining Sklar's and Bayes' theorems, leading to the following results:

$$F_{H_i|T_{i-1}}(h_i|t_{i-1}) = \frac{C\left(F_{H_i}(h_i), F_{T_{i-1}}(t_{i-1})\right)}{F_{T_{i-1}}(t_{i-1})} \tag{3.18}$$

$$F_{T_i|H_{i-1}}(t_i|h_{i-1}) = \frac{C\left(F_{T_i}(t_i), F_{H_{i-1}}(h_{i-1})\right)}{F_{H_{i-1}}(h_{i-1})} \tag{3.19}$$

$$F_{H_{i-1}|T_{i-1}}(h_{i-1}|t_{i-1}) = \frac{C\left(F_{H_{i-1}}(h_{i-1}), F_{T_{i-1}}(t_{i-1})\right)}{F_{T_{i-1}}(t_{i-1})} \tag{3.20}$$

$$F_{T_{i-1}|H_{i-1}}(t_{i-1}|h_{i-1}) = \frac{C\left(F_{T_{i-1}}(t_{i-1}), F_{H_{i-1}}(h_{i-1})\right)}{F_{H_{i-1}}(h_{i-1})} \tag{3.21}$$

Due to the time-reversibility property of a Markov process, the numerators of the equations (3.18) and (3.19) are equal. Regarding their calculation, the Gaussian copula was deployed once again as it was found to provide more accurate results (Anastopoulos et al., 2016). For the same reason, the Clayton copula was chosen for the calculation of the numerators of equations (3.13), (3.20) and (3.21):

$$C(u, v) = (u^{-c} + v^{-c} - 1)^{-1/c} \tag{3.22}$$

where c is the correlation parameter.

In the above, it was preferred to describe the method using probability distribution functions so as to provide more compact closed forms. Despite that, reformulation in terms of probability density functions is straightforward (Anastopoulos et al., 2016).

3.2.3 Marginal distributions

Below we present the formulas of the marginal distributions appearing in equations (3.18) - (3.21). According to Anastopoulos et al. (2016), the specific distributions produce more accurate results when applied in the calculation scheme described in the above.

From a number wave height distributions found in the literature (e.g., Longuet-Higgins, 1952; Næss, 1985; Tayfun, 1990; Boccotti, 2000), the model of Longuet-Higgins (1952) is selected:

$$F_{H_i}(h_i) = 1 - exp\left(-\frac{{h_i}^2}{8m_0}\right) \tag{3.23}$$

where h_i is the wave height and m_0 is calculated by the following equation:

$$m_j = \int_0^\infty \omega^j S(\omega) d\omega \tag{3.24}$$

where m_j is the j^{th} moment of the frequency spectrum S.

Regarding the distribution of the wave periods, the model of Myrhaug & Rue (1998) provided the best fit, compared to the distributions proposed by Longuet-Higgins (1975, 1983), Cavanie et al. (1976) and Bretschneider (1959), to the data obtained from a record of 6353 individual waves in the Norwegian continental shelf:

$$F_{T_i}(t_i) = 1 - exp\left(-\left(\frac{t_i}{T_m}\right)^4\right) \tag{3.25}$$

where $T_m = 2\pi m_0/m_1$ is the mean spectral period and m_0, m_1 are the spectral moments defined from equation (3.24).

3.2.4 Correlation parameters

In this section, the calculation of the copula parameters ρ and c, appearing in the Gaussian and Clayton copulas, respectively, is related to the evaluation of rank correlation coefficients. The latter express the degree of correlation between two variables that are monotonically, but not necessarily linearly, correlated. Anastopoulos et al. (2016) notice that consecutive wave heights are almost linearly correlated and thus, Pierson's linear correlation coefficient is a reasonable choice to describe their relationship. However, wave periods do not follow the same trend and employing linear correlation coefficients may not be appropriate (e.g., Rodriguez & Guedes Soares, 2001). For the above reasons, the correlation coefficient that was chosen for the present analysis is Kendall's τ, defined as:

$$\tau = \frac{c_1 - d_1}{c_1 + d_1} \tag{3.26}$$

where c_1 is the number of concordant pairs and d_1 is the number of discordant pairs from a sample of n observations of two random variables (X, Y). The concordant and discordant pairs are defined as: let (x_1, y_1) and (x_2, y_2) be two sets of observations of the random variables X and Y, respectively. These pairs are said to be concordant if the ranks of both elements agree, i.e., if $x_1 < x_2$ and $y_1 < y_2$ or $x_1 > x_2$ and $y_1 > y_2$. In the opposite case, the pairs are said to be in discordant.

The interesting thing about Kendall's τ is that it is also related to the theory of copula distributions by the following equation (Schweizer & Wolff, 1981):

$$\tau = 4 \iint_{I^2} C(u, v) dC(u, v) - 1 \tag{3.27}$$

where C is the copula distribution. Specifically in the cases of the Gaussian and Clayton copulas, respectively, we obtain:

$$\rho = \sin\left(\frac{\pi}{2}\tau\right) \tag{3.28}$$

$$c = \frac{2\tau}{1-\tau} \tag{3.29}$$

3.3 Time-continuous representation of wave groups

In this section we describe the method for constructing time-continuous wave group profiles related to the "most expected" height and period sequences deriving from the previous analysis. First, we briefly review the approach proposed by Anastopoulos et al. (2016), which deploys the Karhunen-Loève theorem according to the solution given in Sclavounos (2012). However, for some applications, this scheme becomes very computationally expensive, due to the complexity of the Karhunen-Loève solution. This was the motivation to develop an alternative method in terms of Fourier series, presented also below.

3.3.1 The Karhunen-Loève approach

Sclavounos (2012) describes a method for the stochastic representation of ocean waves based on the Karhunen-Loève theorem. The advantage of the method lies in the fact that it allows for the representation of the wave field with the minimum number of independent sources of uncertainty (often an order of magnitude less than the traditional representation in terms of Fourier series).

According to the theorem, if $\eta(x,t)$ is a stochastic signal (in this case the water surface elevation) defined over a finite time interval $(-T,T)$, then it accepts the following expansion:

$$\eta(x,t) = \sum_{n=0}^{\infty} a_n f_n(x,t), \quad -T < t < T \tag{3.30}$$

where a_n are independent random variables and f_n are the basis functions. The latter are the solution of the integral equation:

$$\int_{-T}^{T} R(t-\tau) f_n(t) d\tau = \kappa_n f_n(t) \tag{3.31}$$

with R being the autocorrelation function of η and κ_n being the eigenvalues of the orthogonal functions f_n. The solution of the above equation is a complex task. Slepian and Pollack (1961) observed that there exists an explicit solution when the kernel of equation (3.31) is the $sinc$ function[3]. In this case, the eigenfunctions turn out to be the Prolate Spheroidal Wave Functions ($PSWFs$). Sclavounos (2012) took advantage of the similarities between the $PSWFs$ and the autocorrelation function that describes wind generated waves to propose an efficient method to calculate the basis functions. The same method was used in Anastopoulos et al. (2016) for the time-continuous representation of the "most expected" irregular wave groups.

3.3.2 A new method using Fourier series

A Fourier series is an expansion of a periodic function f in terms of infinite sums of sines and cosines:

$$\begin{aligned} f(x) &= a_o + \sum_{n=1}^{\infty} a_n \cos(nx) + b_n \sin(nx) \\ &= a_0 + a_1 cosx + a_2 \cos(2x) + a_3 \cos(3x) + \cdots \\ &\quad + b_1 sinx + b_2 sin2x + b_3 sin3x + \cdots \end{aligned} \tag{3.32}$$

where the calculation of the basis coefficients a_n and b_n is based on the orthogonality relationships of the sine and cosine functions.

In the same spirit, one can express the water elevation $\eta(x,t)$ as (Longuet-Higgins, 1952):

[3] i.e., the function $\frac{\sin(x)}{x}$

$$\eta(x,t) = \sum_{n=1}^{\infty} a_n \cos(k_n x + \omega_n t + \varepsilon_n) \tag{3.33}$$

where k_n is the wave number, ω_n is the angular frequency and ε_n are random phases, uniformly distributed in $[0,2\pi)$. In the above form, we have assumed that waves propagate along the negative x'x direction. Since we are interested in the study of ship roll motions, we assume that $x = 0$. So, equation (3.33) becomes:

$$\eta(t) = \sum_{n=1}^{\infty} a_n \cos(\omega_n t + \varepsilon_n) \tag{3.34}$$

By elaborating on equation (3.34) we end up with a form similar to equation (3.32):

$$\begin{aligned} \eta(t) &= \sum_{n=1}^{\infty} a_n [\cos(\omega_n t)\cos(\varepsilon_n) - \sin(\omega_n t)\sin(\varepsilon_n)] \\ &= \sum_{n=1}^{\infty} a_n \cos(\varepsilon_n)\cos(\omega_n t) - a_n \sin(\varepsilon_n)\sin(\omega_n t) \end{aligned} \tag{3.35}$$

We opt for a wave group representation in terms of odd basis functions so that the wave group signal always starts at t_0 with a zero up-crossing; thus, $\eta(t_0) = 0$. Consequently, the $cos(\cdot)$ terms in equation (3.35) can be omitted:

$$\eta(t) = -\sum_{n=1}^{\infty} a_n \sin(\varepsilon_n)\sin(\omega_n t) \tag{3.36}$$

According to the "theory of sea states" we know that (Boccotti, 2000):

$$S(\omega)d\omega = \sum_i \frac{1}{2} {a_i}^2 \tag{3.37}$$

where a_i are amplitudes for i such that $\omega - \frac{d\omega}{2} < \omega_i < \omega + \frac{d\omega}{2}$ (see Figure 3.2).

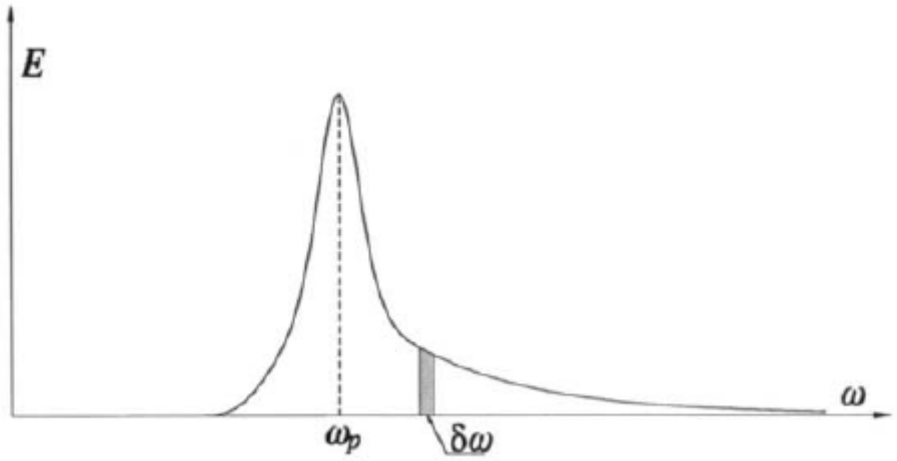

Figure 3.2 Definition of spectrum: the shaded area is equal to the partial sum $\sum_i \frac{1}{2} {a_i}^2$ (Boccotti, 2000)

The coefficients a_n can be written in terms of the wave energy spectrum as:

$$a_n = \sqrt{2S(\omega_n)d\omega} \tag{3.38}$$

Since the characteristics[4] of a wave group under construction are known from the application of the iterative scheme of equations (3.6)-(3.7), one can calculate the terms $\sin(\varepsilon_n)$ from the solution of an interpolation problem that is formulated using the wave group characteristics as constraints in equation (3.36).

Let t_i be the instant when the wave with height H_i and period T_i has a zero up-crossing. The following constraints are imposed:

[4] i.e., wave heights, periods and run length.

$$\eta(t_i) = 0$$
$$\eta\left(t_i + \frac{T_i}{4}\right) = \frac{H_i}{2}$$
$$\eta\left(t_i + \frac{3T_i}{4}\right) = -\frac{H_i}{2}$$
$$\left.\frac{d\eta}{dt}\right|_{t=t_i+\frac{T_i}{4}} = 0$$
$$\left.\frac{d\eta}{dt}\right|_{t=t_i+\frac{3T_i}{4}} = 0 \qquad (3.39)$$

For a wave group with j number of waves, a system of $5j$ equations and $5j$ components in equation (3.36) should have a unique solution. However, since we have included only the $sin(\cdot)$ terms of the Fourier series, $\eta(t_0) = 0$ (with t_0 being the time instant of the beginning of the wave group) is always satisfied and thus, the first constraint of equation (3.39) can be omitted in the case of the first wave of the group. In addition, the fact that the $sin(\cdot)$ functions are periodic allows for further component reduction: the "most expected" height and period sequences derived from the method of Anastopoulos et al. (2016) are symmetric with respect to the central wave and thus, it is sufficient to apply the above constraints only to the first half of the wave group duration. The second half will be just the reflection of the first half, produced due to the periodicity of the $sin(\cdot)$ functions. Under these terms, we select to truncate the series expansion in equation (3.36) at $n = (5j-1)/2$ (see Figure 3.3):

$$\eta(t) = -\sum_{n=1}^{(5j-1)/2} \sin(\varepsilon_n)\sqrt{2S(\omega_n)d\omega_n}\,\sin(\omega_n t) \qquad (3.40)$$

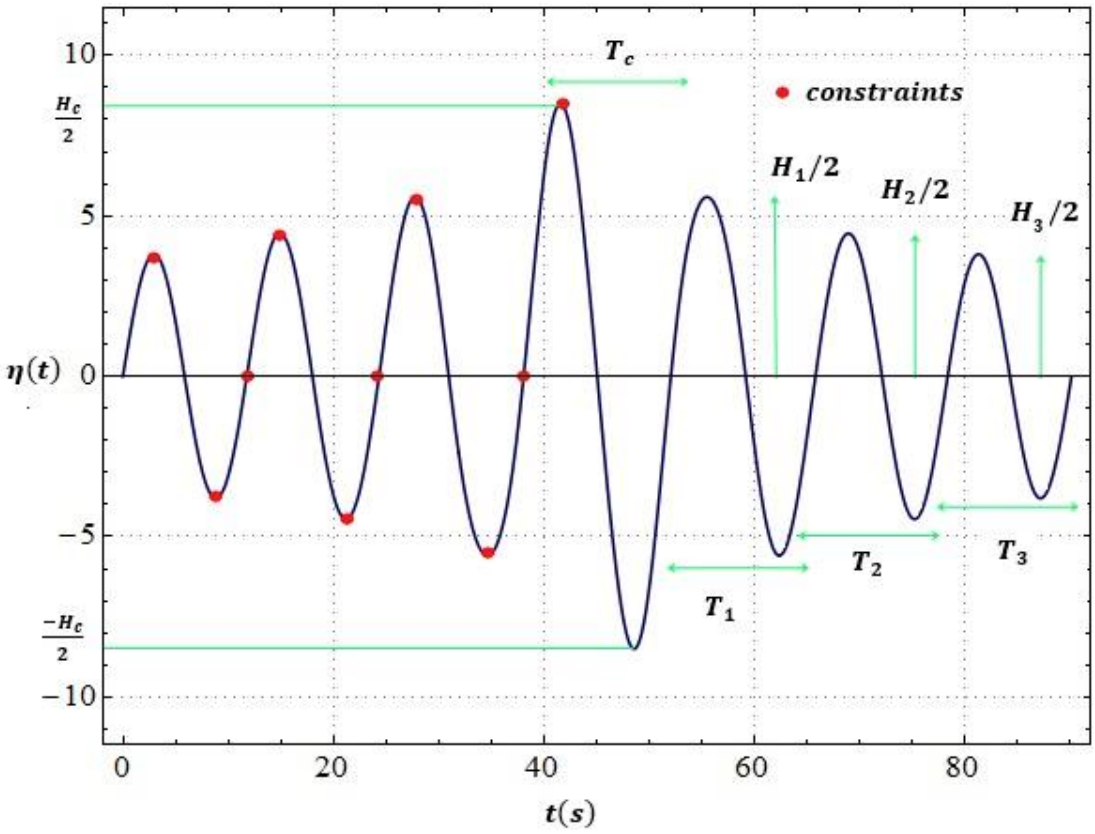

Figure 3.3 Illustration of wave group construction process

4. Mathematical model of roll motion in beam seas

4.1 Introduction

In this chapter we describe the mathematical model of roll motion that will be used to identify the "critical wave groups" in the deterministic part of the method.

Several models have been developed for simulating ship motions, being available to the designer in the form of commercial software packages. Different models are suitable for different applications and often more than one tool is deployed by the designer, depending on the simplifications the model is based on as well as the desired accuracy at the particular stage of the design process.

Potential flow theory is widely used in the study of irrotational, incompressible and inviscid flows with viscosity effects considered to a limited extent through correction schemes. Other approaches target the solution of the Navier-Stokes equations to model the corresponding hydromechanical pressure forces. In such case, equations of motion are solved by time-domain codes, leading to accurate results even in the case of complex hulls, yet with high computational cost.

In general, forces of different nature act upon the hull of a vessel and are usually classified in the following categories:

1. Hydrostatic forces also known as restoring forces
2. Incident wave induced forces which are the forces due to the undisturbed wave
3. Diffraction forces which are the forces generated from the diffraction of the incident wave due to the presence of the ship
4. Radiation forces which are forces generated by the movement of the ship and are also known as hydrodynamic forces of added mass and damping
5. Viscous forces due to viscous flow effects
6. Other forces such as aerodynamic forces due to the wind

In the present thesis, ship roll motion is studied using a single Degree Of Freedom (DOF) model with nonlinear restoring and damping terms. The analysis is based on the pioneering work of Froude in the 1870s. Even though more sophisticated hydrodynamic models have been developed ever since, this model remains popular because it allows for a deeper

understanding of the nonlinear dynamic response of the vessel as well as the effect of the different parameters involved in the problem (Spyrou NTUA, 2014).

4.2 Mathematical model of uncoupled roll motion

The model is based on the Froude-Krylov assumption which states that the ship is sufficiently small so that it does not disturb the pressure field of the incident waves. In other words, diffraction effects are insignificant. The assumption is more consistent when the ratio of the wavelength λ to the ship's beam B takes large values (i.e., λ/B > 5). In such case, the ship follows the rotational motion of the water particles giving rise to the concept of the "effective gravitational field" where the effective gravity acts always perpendicular to the instantaneous water surface.

Depending on the type of assessment, roll motion can be studied with respect to different angle definitions. For example, if one is interested in the study of inertial forces that cause cargo shift, the absolute transverse rolling angle χ (defined by the centerline perpendicular to the ship deck when the ship is rolling and the line perpendicular to the calm level of the sea) should be considered. On the other hand, if one is interested in avoiding capsize then the relative rolling angle φ (defined by the centerline perpendicular to the ship deck when the ship is rolling and the line perpendicular to the wave slop at midship) should be considered (see Figure 4.1).

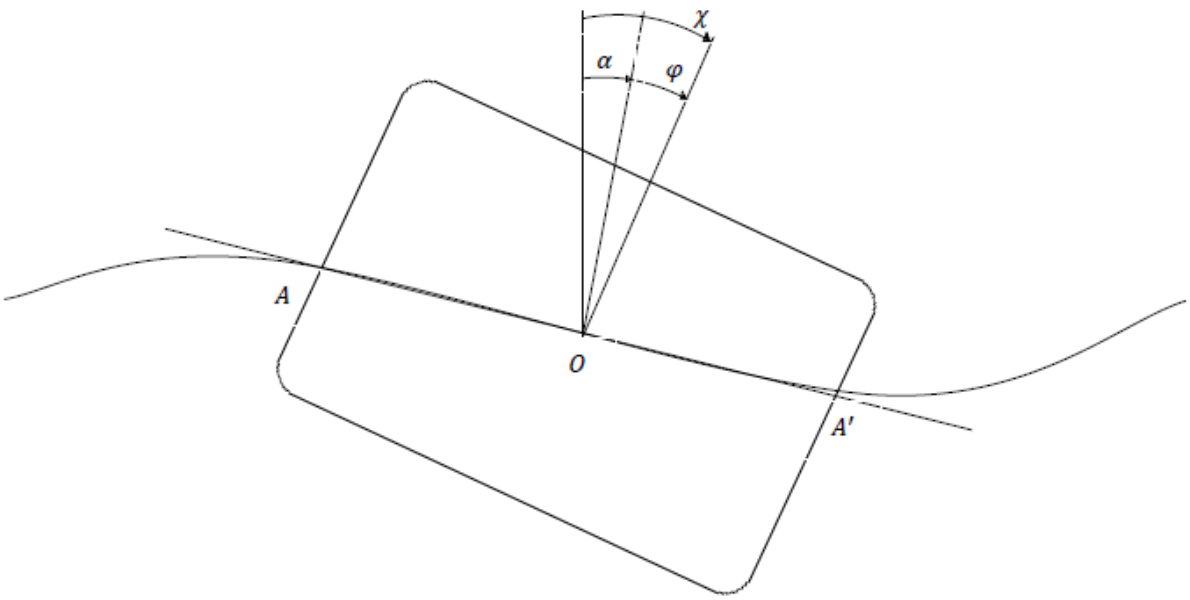

Figure 4.1 Ship rolling in beam seas (Anastopoulos diploma thesis, 2012)

Below we derive the equation of roll motion by employing Newton's Second Law (Spyrou, NTUA 2014):

$$I\ddot{\chi} = -\delta I(\ddot{\chi} - \ddot{a}) - D(\dot{\varphi}) - R(\varphi) \tag{4.1}$$

where I is the roll moment of inertia, δI is the added mass which is the moment of inertia added to the system due to the acceleration of the surrounding water dragged by the ship, D is the damping moment, R is the restoring moment and a is the instantaneous wave slope at the middle of the ship, defined as:

$$a = \frac{\partial \eta(x,t)}{\partial x} \tag{4.2}$$

where $\eta(x,t)$ is the water surface elevation.

Considering that $\chi = \varphi + a$ equation (4.1) takes the following final form:

$$(I + \delta I)\ddot{\varphi} + D(\dot{\varphi}) + R(\varphi) = -I\ddot{a} \tag{4.3}$$

4.2.1 Restoring moment

By assuming that the wave length is large compared to the beam of the ship the waterline AOA' can be approximated by a straight line (Figure 4.1). In addition, the isobars of hydrodynamic pressure at the point where the wave is displaced by the ship's hull do not differ much from a hydrostatic condition. Thus, the restoring moment can be expressed by the following equation:

$$R(\varphi) = \Delta g GZ(\varphi) \tag{4.4}$$

where Δ is the displacement of the ship, g is the gravitational acceleration and $GZ(\varphi)$ is the righting arm in calm water.

4.2.2 Damping moment

Roll damping emerges from fluid viscosity and energy loss due to the waves generated by the forced oscillation of the vessel (also known as radiation damping). Usually, the latter is the main source of damping in pitch, heave, sway and yaw motions and thus, potential flow theory can be employed with fairly good accuracy. However, the same does not apply in the case of roll motion because the radiation component is only a small portion of the total damping.

A method that is widely used for the calculation of roll damping is the so called "Ikeda's method", described in Ikeda et al. (1978). The method provides semi-empirical formulas for the calculation of an "equivalent damping coefficient" B_{eq} defined as the sum of different damping components:

$$B_{eq} = B_f + B_e + B_w + B_L + B_{BK} \tag{4.5}$$

where B_F, B_E B_W, B_L and B_{BK} are damping coefficients due to skin friction, eddy shedding, wave making, lift and bilge keels effects, respectively, as illustrated in Figure 4.2. The damping components in equation (4.5) are treated separately, neglecting any possible interaction among them. Despite that contemporary methods have been developed for more accurate calculation of the roll damping moment (e.g., Computational Fluid Dynamics – CFD methods), "Ikeda's method" remains popular due to its simplicity and applicability even in the preliminary stages of the design process.

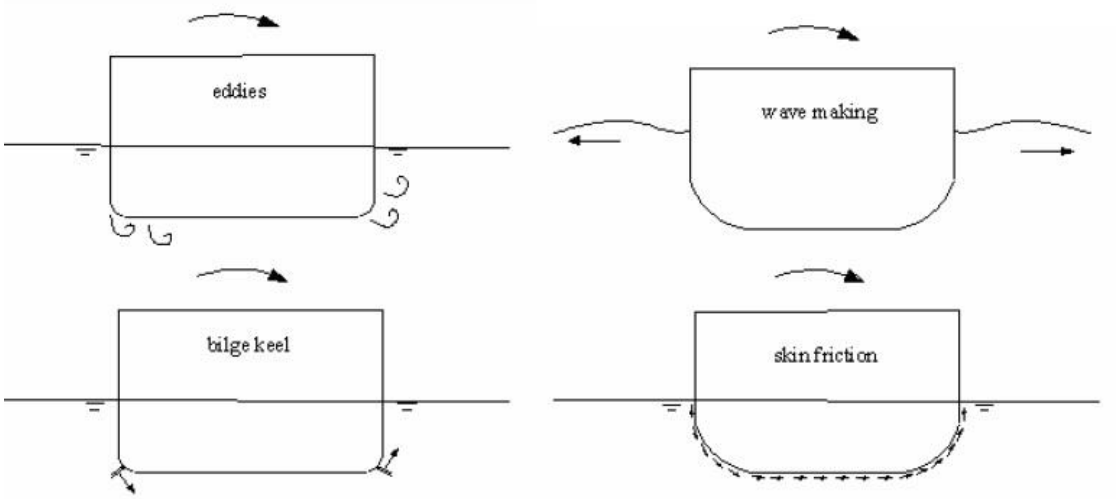

Figure 4.2 Roll damping components (Themelis PhD thesis, 2008)

In the current thesis the damping moment is modelled as:

$$D(\dot{\varphi}) = B_1\dot{\varphi} + B_2\dot{\varphi}|\dot{\varphi}| \tag{4.6}$$

where B_1, B_2 are constant terms related to the "equivalent linear damping" coefficient B_{eq} through the following equation (Ikeda et al., 1978):

$$B_{eq} = B_1 + \frac{8\alpha\omega}{3\pi}B_2 \tag{4.7}$$

where α and ω are the roll amplitude and frequency, respectively.

Equation (4.7) derives from:

$$2\int_{-\varphi}^{\varphi} B_{eq}\dot{\varphi}d\varphi = 2\int_{-\varphi}^{\varphi}(B_1\dot{\varphi} + B_2\dot{\varphi}|\dot{\varphi}|)d\varphi \tag{4.8}$$

by considering that the energy loss during one roll period is the same for both the equivalent linear damping moment and the actual nonlinear damping moment.

5. Application of the methodology

In this chapter the "critical wave groups" method is applied on a modern containership to evaluate its roll dynamic stability in a specific sea state. In more detail, both regular and the "most expected" wave group profiles, deriving from the procedure described in Chapter 3 are employed and the critical wave groups are identified in terms of heights, periods and run length, using the mathematical model of roll motion, presented in Chapter 4. In the probabilistic part of the approach, the probability that the vessel exceeds several angle thresholds is computed. Desirable distributions of wave heights and periods are obtained from Monte Carlo simulations of the wave field in order to eliminate the uncertainty related to the accuracy of the "spectral methods" that are used in the original formulation of the method (Themelis & Spyrou, 2007). In addition, the copula parameters, involved in the calculation of the "most expected" height and period sequences, are obtained from the same data using equations (3.26), (3.28) and (3.29). The results of both cases are validated by direct Monte Carlo simulations of roll motion. The method was implemented using the *Wolfram Mathematica* programming software.

5.1 Monte Carlo simulations of the wave field

The distribution of interest, involved in the calculation of the probability of encountering any wave group higher than the critical, concerns the heights and periods of successive waves and it is denoted as $f_{H_i,T_i,H_{i-1},T_{i-1}}$. At the same time, we want to calculate the Gaussian and Clayton copula parameters, given in equations (3.28) and (3.29), to produce the transition probabilities of equations (3.6) and (3.7). The above are extracted from Monte Carlo simulations of the water surface elevation, performed using the following stochastic model (Longuet-Higgins, 1952):

$$\eta(x,t) = \sum_{n=1}^{N} \sqrt{2S(\omega_n)d\omega_n}\cos(k(\omega_n)x + \omega_n t + \varepsilon_n) \qquad (5.1)$$

where S is the wave spectrum, k is the wave number, ε_n is a random phase, ω_n is the angular frequency, $d\omega$ is the resolution in the frequency domain and N is the number of components used to discretize the spectrum S. According to the dispersion relationship and assuming that the water is deep, the wave number is equal to:

$$k(\omega_n) = \frac{{\omega_n}^2}{g} \tag{5.2}$$

where g is the gravitational acceleration. The phases ε_n are uniformly distributed in $[0,2\pi)$ and the frequency domain resolution $d\omega$ is equal to:

$$d\omega = \frac{\Omega_{max} - \Omega_{min}}{N-1} \tag{5.3}$$

where Ω_{max} and Ω_{min} define the spectral bandwidth, being the maximum and minimum assumed frequencies, respectively.

For this application, the JONSWAP spectrum was used (Hasselmann et al., 1973):

$$S(\omega) = Ag^2\omega^{-5}e^{-\frac{5}{4}\left(\frac{\omega}{\omega_p}\right)^{-4}}\gamma^{e^{-0.5\left(\frac{\omega-\omega_p}{\sigma\omega_p}\right)^2}} \tag{5.4}$$

where g is the gravitational acceleration, ω is the angular frequency, $\omega_p = 2\pi/T_p$ is the peak angular frequency and T_p the peak period, γ is the JONSWAP peakness parameter, σ is the JONSWAP shape parameter and A is the Phillips parameter:

$$\gamma = \begin{cases} 5, if\ \dfrac{T_p}{\sqrt{H_s}} \leq 3.6 \\ exp\left(5.75 - 1.15\dfrac{T_p}{\sqrt{H_s}}\right), if\ 3.6 \leq \dfrac{T_p}{\sqrt{H_s}} \leq 5 \\ 1, if\ 5 \leq \dfrac{T_p}{\sqrt{H_s}} \end{cases} \tag{5.5}$$

$$\sigma = \begin{cases} 0.07, if\ \omega \leq \omega_p \\ 0.09\ if\ \omega > \omega_p \end{cases} \tag{5.6}$$

$$A = \frac{5}{16}\frac{{H_s}^2{\omega_p}^4}{g^2}A_\gamma \tag{5.7}$$

where H_s is the significant wave height and A_γ the JONSWAP normalizing factor:

$$A_\gamma = 1 - 0.287\ln(\gamma) \tag{5.8}$$

The simulations were conducted for $H_s = 10m$ and $T_p = 13.6s$ which is close to the roll natural period of the vessel. The computed wave spectrum is shown in Figure 5.1.

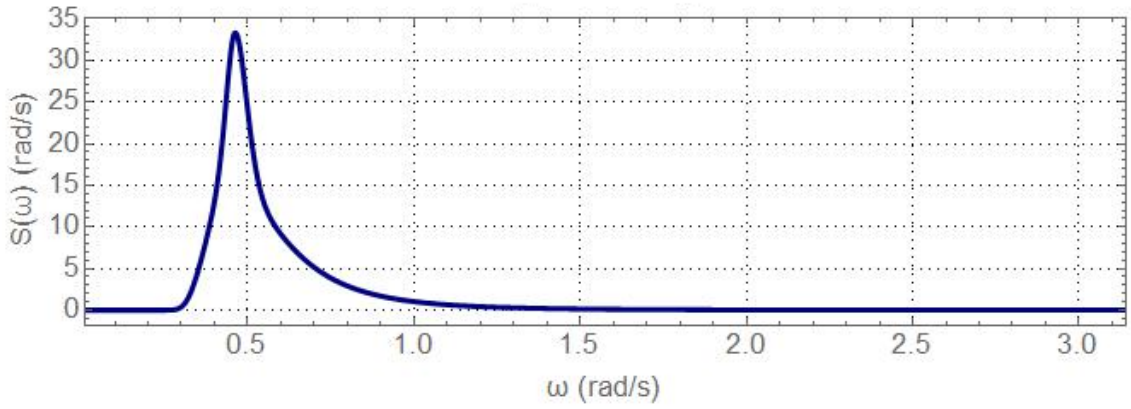

Figure 5.1 JONSWAP spectrum density function for $H_s = 10m$ and $T_p = 10s$

In total, 81884 waves were analyzed from 10 realizations that were produced, each having a duration of $86400\,sec\,(24\,hours)$ with $\Omega_{max} = 2.002\,rad/s$, $\Omega_{min} = 0.002\,rad/s$, $N = 55010$, $d\omega = 0.000036357\,rad/s$ and $\Delta t = 0.1s$. Figure 5.2 shows a time record of equation (5.1).

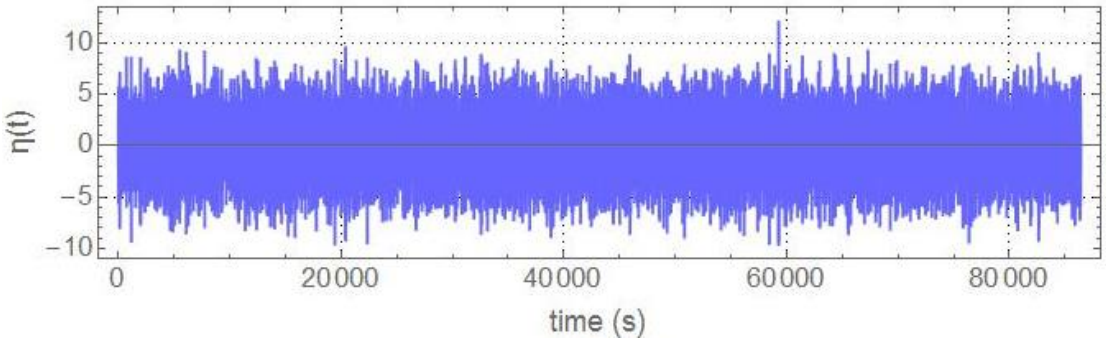

Figure 5.2 Time record of the water surface elevation

5.2 Irregular wave group construction

5.2.1 Correlation parameters

The correlation parameters of the Gaussian and Clayton copulas, presented in Chapter 3, were calculated from the results of the Monte Carlo simulations of the wave field, described above. Specifically, Kendall's τ was calculated using equation (3.26) and the results are given in Table 5.1, below. Finally, equations (3.28) and (3.29) were employed to finalize the calculations. The results are shown in Table 5.2. The index i is used to distinguish the present state (height or period) from the previous one, denoted by $i-1$.

Table 5.1 Calculated correlation coefficients

$\tau_{H_{i-1}T_{i-1}} = 0.443$	$\tau_{T_{i-1}H_i} = 0.213$
$\tau_{H_{i-1}H_i} = 0.249$	$\tau_{T_{i-1}T_i} = 0.199$

Table 5.2 Calculated copula correlation parameters

$c_{H_1T_1} = 1.597$	$\rho_{T_1H_2} = 5.840 \cdot 10^{-3}$
$\rho_{H_1H_2} = 6.826 \cdot 10^{-3}$	$\rho_{T_1T_2} = 5.456 \cdot 10^{-3}$

5.2.2 Marginal distributions

The next step is to compute the marginal probability distributions appearing in equations (3.18)-(3.21). To this end, the models of equations (3.23) and (3.25) are employed. In Figure 5.3 the model of Longuet-Higgins (1952) for the probability density function (pdf) of wave heights is tested against the experimental pdf computed from the water surface elevation data. As we can see, equation (3.23) agrees with the data fairly well.

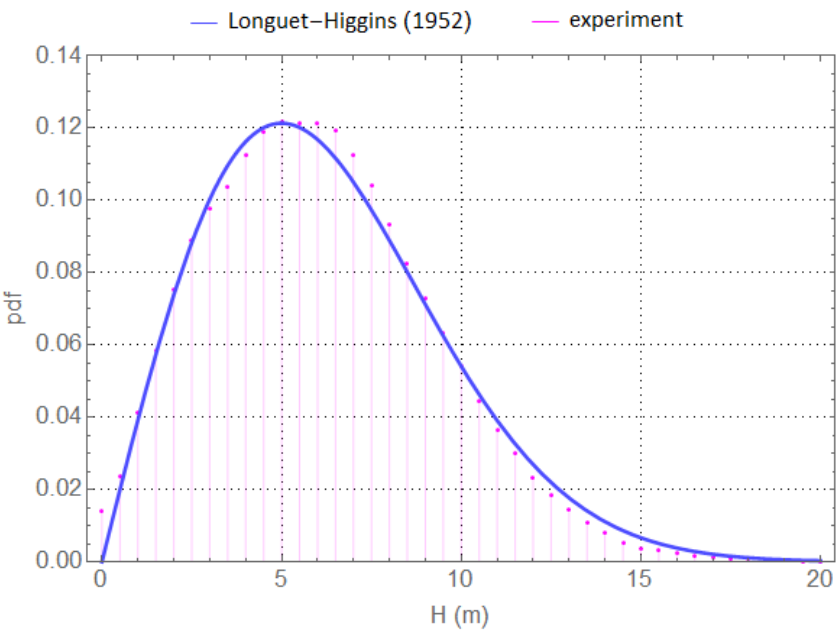

Figure 5.3 Theoretical and experimental pdfs of wave heights

In the same spirit, in Figure 5.4 the distribution proposed by Myrhaug & Rue (1998) is compared to the distribution of wave periods obtained from the Monte Carlo simulations. As we can see it is not very accurate, especially in the region of the mean spectral period $T_m = 11.05\ sec$.

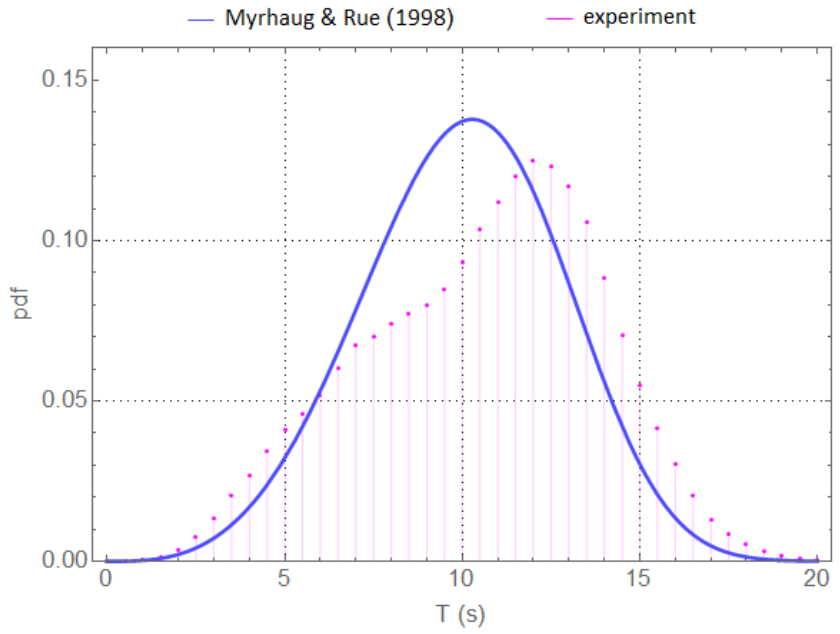

Figure 5.4 Theoretical and experimental pdfs of wave periods

5.2.3 Copula distributions

Based on the above, we compute the copula density functions involved in the definition of the transition probabilities of equations (3.6) and (3.7). In more detail, given the marginal distributions and the correlation parameters, the distributions in equations (3.18)-(3.21) are computed. Next, we compute the distributions in equations (3.12) and (3.14) and finally, we can compute the distribution in equation (3.13).

As a preliminary investigation, experimental joint probability density functions, obtained from the Monte Carlo simulations of the water surface elevation are compared to the copula pdfs of equations (3.12), (3.14), (3.18) & (3.21). The results are given in the Figure 5.5, (a)-(d), respectively. As we can see, the selected copula models capture the qualitative features of the experimental data.

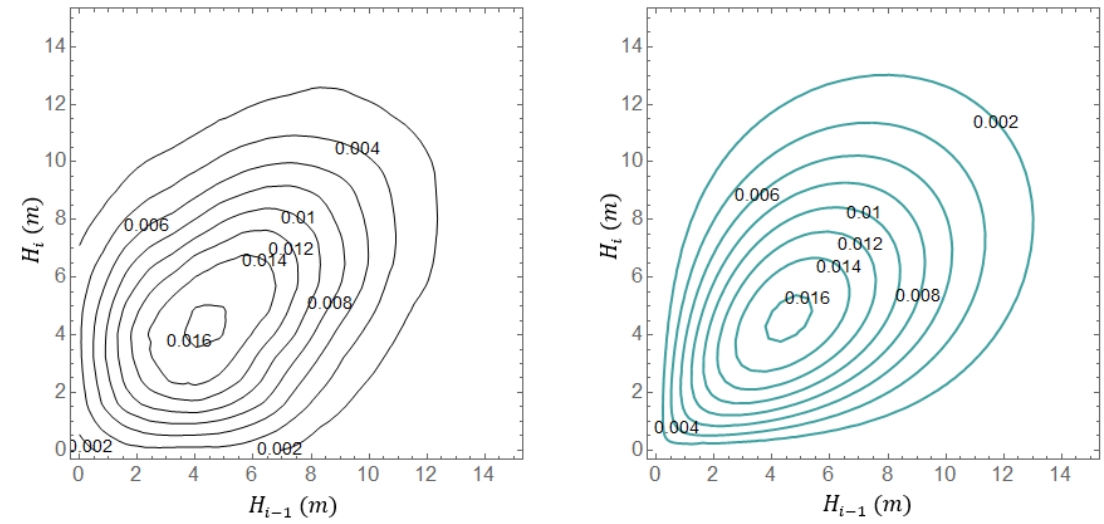

a e

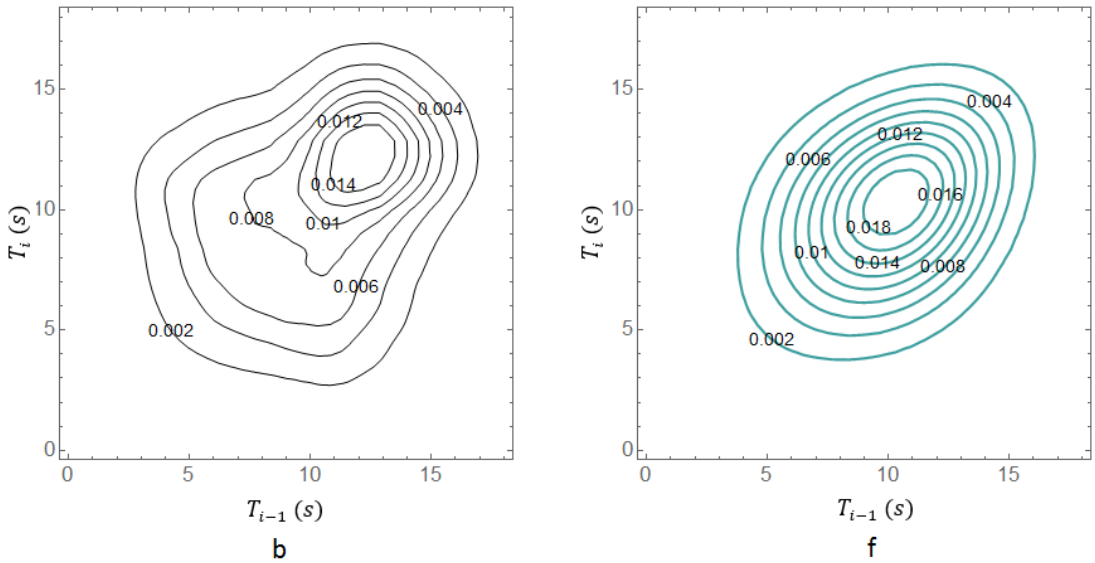

b f

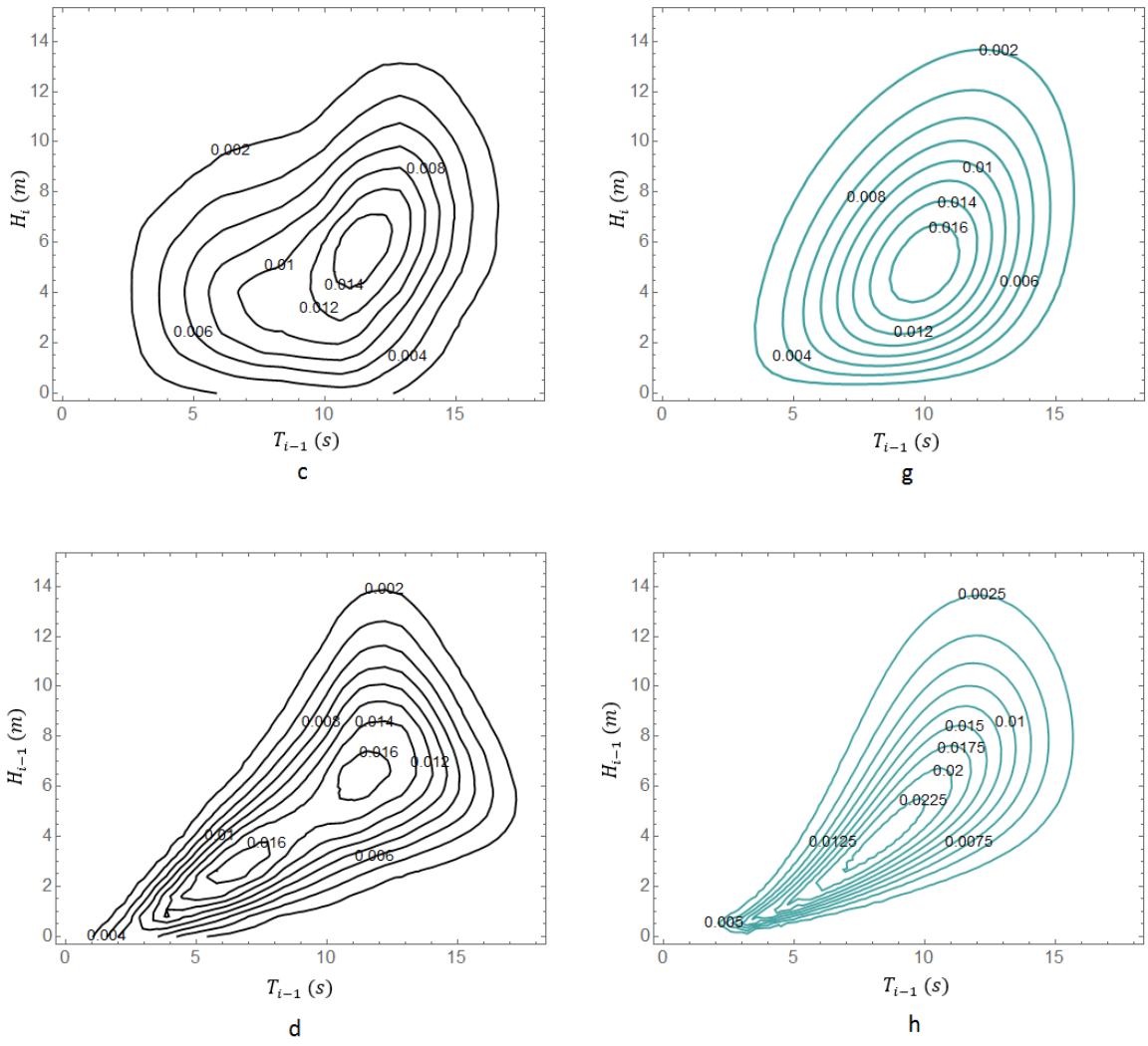

Figure 5.5 [a, b, c, d]: experimental joint pdfs [e, f, g, h]: copula pdfs

5.2.4 Constructed wave groups

After computing the transition probabilities of equations (3.6) and (3.7) we can generate the "most expected" height and period sequences by specifying the height and period of the central wave. Then, equation (3.40) is employed to construct the continuous-time counterparts of these sequences. The method is demonstrated in Figure 5.6 and Figure 5.7, illustrating derived irregular wave groups with run length $j = 5$ waves. In the former, cases with fixed central wave period $T_c = 14s$ and increasing central wave heights are presented, while in the latter, the period of the central wave varies and the central wave height is fixed at $H_c = 17m$. The values of the heights and periods of the individual waves are given in Table 5.3 and Table 5.4.

Table 5.3 Heights and periods of the constructed wave groups with run length $j = 5$, central wave period $T_c = 14s$ and variable central wave heights

Tc=14s											
H-2	8.5 m	T-2	12.3 s	H-2	8.9 m	T-2	12.6 s	H-2	9.3 m	T-2	12.8 s
H-1	10.5 m	T-1	13.4 s	H-1	11.2 m	T-1	13.7 s	H-1	11.9 m	T-1	14.1 s
Hc	**15 m**	**Tc**	**14 s**	**Hc**	**17 m**	**Tc**	**14 s**	**Hc**	**19 m**	**Tc**	**14 s**
H1	10.5 m	T1	13.4 s	H1	11.2 m	T1	13.7 s	H1	11.9 m	T1	14.1 s
H2	8.5 m	T2	12.3 s	H2	8.9 m	T2	12.6 s	H2	9.3 m	T2	12.8 s

Table 5.4 Heights and periods of the constructed wave groups with run length $j = 5$, central wave height $H_c = 17m$ and variable central wave period

Hc=17m											
H-2	8.9 m	T-2	12.6 s	H-2	9.2 m	T-2	12.8 s	H-2	9.6 m	T-2	13 s
H-1	11.2 m	T-1	13.7 s	H-1	11.7 m	T-1	14.1 s	H-1	12.2 m	T-1	14.4 s
Hc	**17 m**	**Tc**	**14 s**	**Hc**	**17 m**	**Tc**	**15 s**	**Hc**	**17 m**	**Tc**	**16 s**
H1	11.2 m	T1	13.7 s	H1	11.7 m	T1	14.1 s	H1	12.2 m	T1	14.4 s
H2	8.9 m	T2	12.6 s	H2	9.2 m	T2	12.8 s	H2	9.6 m	T2	13 s

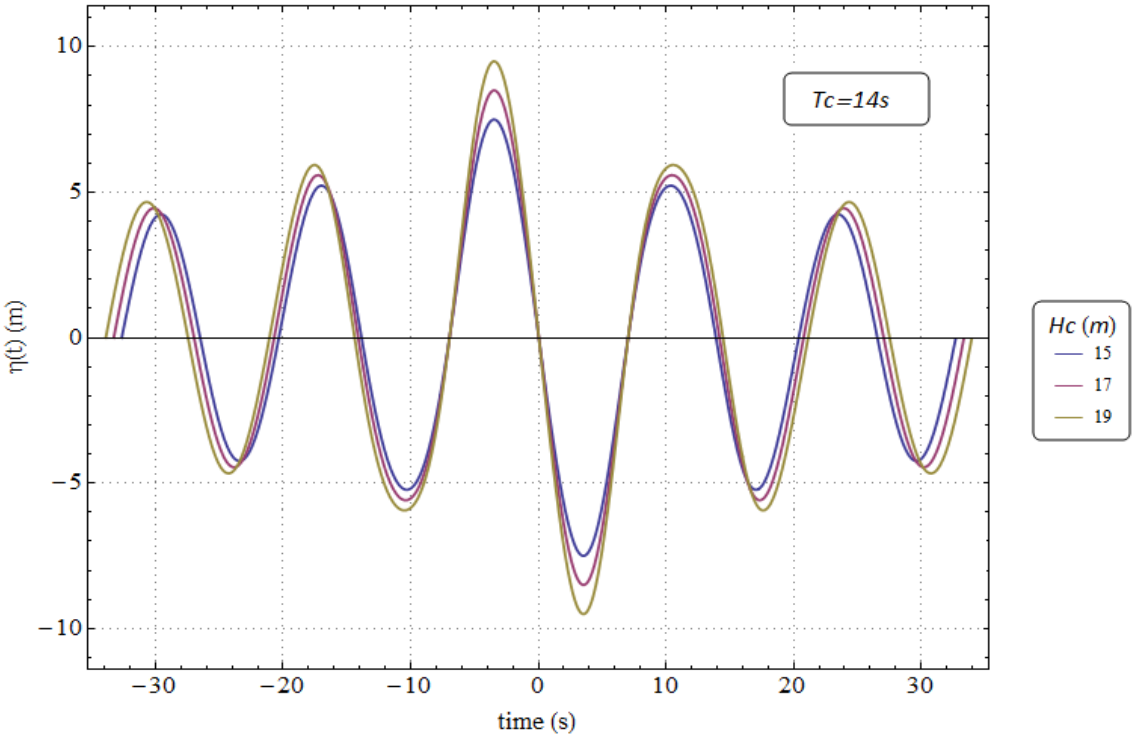

Figure 5.6 Constructed wave groups with run length $j = 5$, central wave period $T_c = 14s$ and varying central wave height

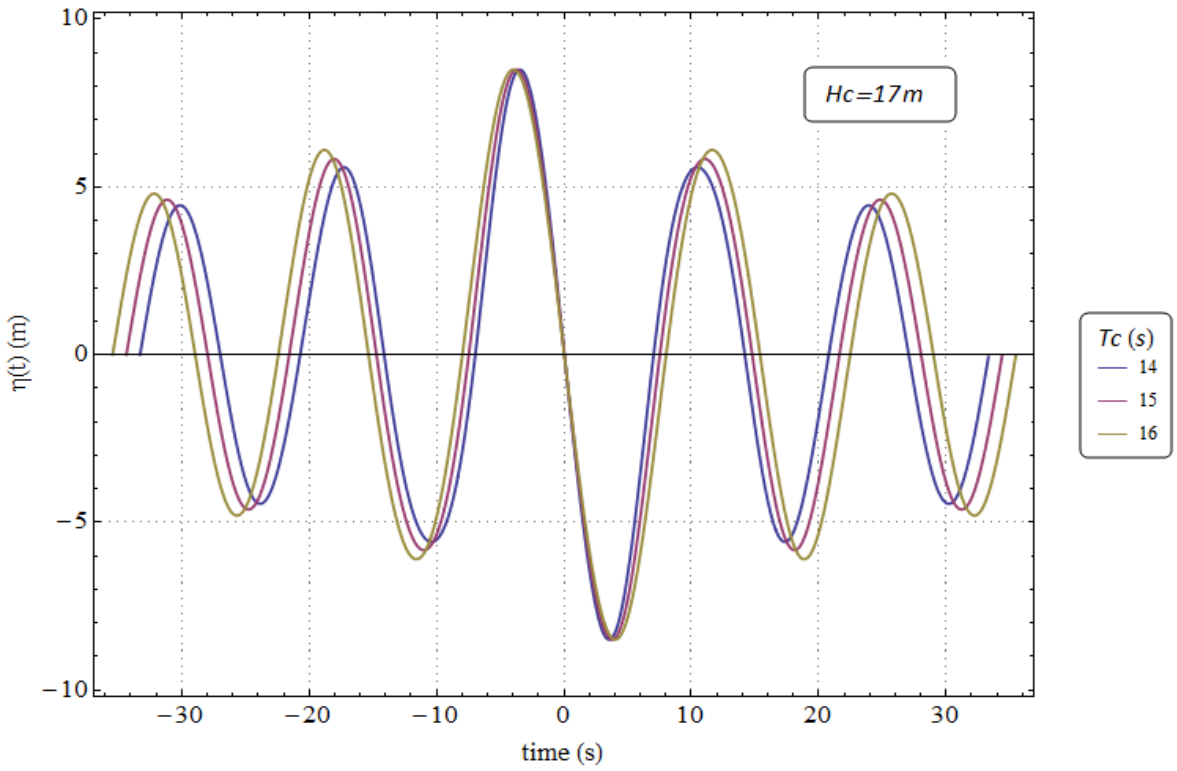

Figure 5.7 Constructed wave groups with run length $j = 5$, central wave height $H_c = 17m$ and varying central wave period

5.3 Deterministic part

In the deterministic part of the "critical wave groups" method, simulations of ship roll motion under wave group excitation are performed, using the mathematical model of Chapter 4. The "critical" wave groups represent thresholds, identified in terms of wave heights, periods and run length.

5.3.1 Ship particulars

The main particulars of the selected containership are presented in the Table 5.5, below. In the context of this thesis only one loading condition is examined which corresponds to the design draught and necessary information was extracted from the loading manual of the ship (see Table 5.6). Moreover, the natural roll period T_0 was calculated from free roll decay numerical experiments using the mathematical model described in Chapter 4. Finally, an illustration of the general arrangement of the vessel is shown in Figure 5.8.

Table 5.5 Basic particulars of the containership

Length overall (L_{OA})	250	M	Draught design (T_d)	11.5	m
Length between perpendiculars (L_{PP})	238.35	M	Block coefficient (C_B)	0.647	
Breadth (B)	37	M	Displacement at T_d (Δ)	68014	t
Depth (D)	19.6	M	Container capacity	4896	TEU

Table 5.6 Loading condition main characteristics

Displacement (Δ)	68199.1	t
Draught (T)	11.52	m
Vertical position of the center of gravity above keel (KG)	14.77	m
Metacentric height corrected (GM)	2.85	m
Natural roll period (T_0)	15.1	sec
Number of containers	2659	
Weight of containers	16	t/TEU

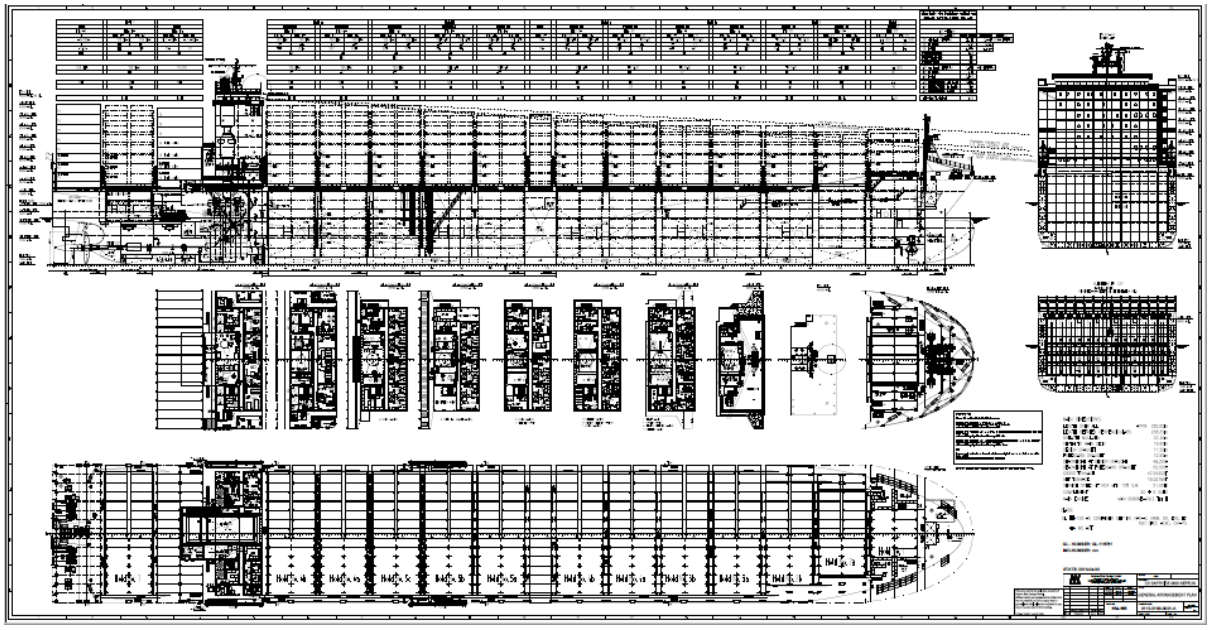

Figure 5.8 General arrangement of the containership

To calculate the roll moment of inertia plus the added mass we used the following equation (Spyrou NTUA, 2012):

$$\omega_0 = \sqrt{\frac{\Delta g GM}{I + \delta I}} \tag{5.9}$$

where ω_0 is the natural angular frequency. Further, we assumed that $\delta I = 0.1\, I$. The damping coefficients were calculated using the simplified method of Ikeda et al. (1978), described in Kawahara et al. (2009). The GZ curve was modelled using a 9th degree polynomial to fit the data provided from the loading manual of the vessel for the specific loading condition (Figure 5.9). Finally, the angle of vanishing stability is $\varphi_v = 65°$.

Table 5.7 Roll model necessary values

Roll moment of inertia (I)	$1.08890 \cdot 10^7$	$t \cdot m^2$
Added mass (δI)	$0.109018 \cdot 10^7$	$t \cdot m^2$
Displacement (Δ)	68199.1	t
Gravitational acceleration (g)	9.81	m^2/s
Damping coefficient (B_1)	655021.45	$t \cdot m^2/s$
Damping coefficient (B_2)	25190.30	$t \cdot m^2/s$

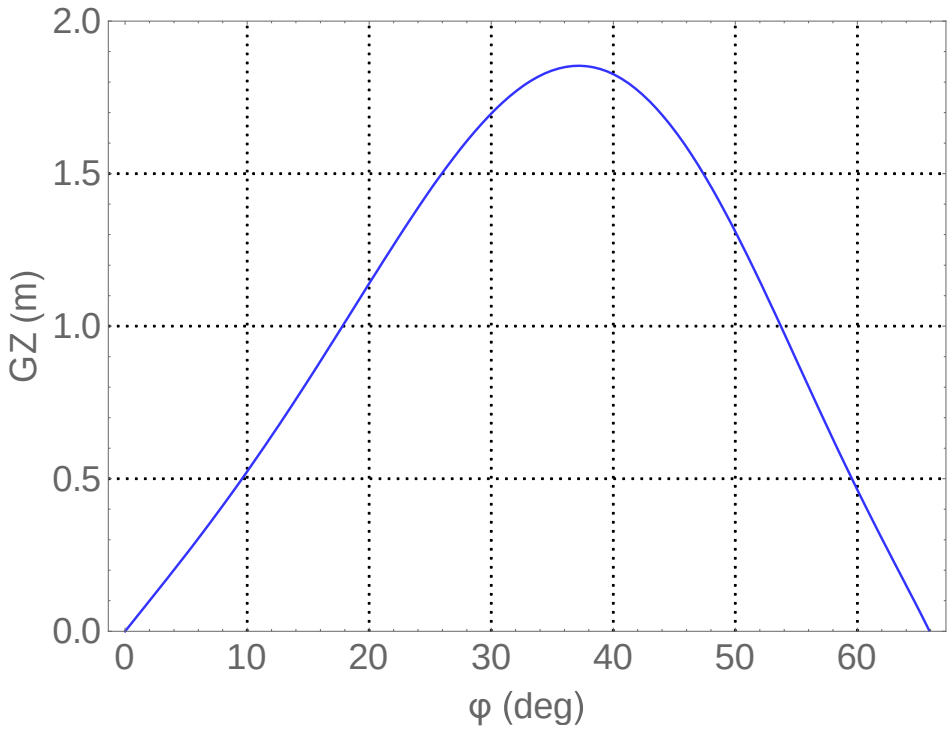

Figure 5.9 Righting lever arm of the container vessel modelled in Mathematica

5.3.2 Critical wave groups

Given the period of a regular wave train and the run length, a "critical" wave group is defined as the wave group that provokes exceedance of a pre-defined roll angle threshold, having the lowest wave height. In more detail, run lengths from 1 to 11 waves were considered with periods spanning the range from 1 to 22 seconds at every 1 second. In any case, wave heights should not exceed the Airy breaking limit (Ochi, 1998):

$$H_{max} = 0.027gT^2 \tag{5.10}$$

where g is the gravitational acceleration and T the wave period. Finally, the wave group profile was modelled as:

$$\eta(x,t) = \frac{H}{2}\sin(kx + \omega t) \tag{5.11}$$

where H is the wave height, k is the wave number and ω is the angular frequency of the wave.

The same logic applies in the case of irregular wave groups. However, an important tuning parameter regarding the generation of the "most expected" wave sequences is the height threshold above which consecutive waves are assumed to be part of the group (Anastopoulos et al., 2016). In this thesis, the root mean square value of the sea state heights was selected: $H_{rms} = H_s/\sqrt{2}$ where H_s is the significant wave height (for the selected sea state $H_{rms} = 7.1m$). Under these terms, the iterative scheme of equations (3.6) and (3.7) is applied until observing a wave with height below H_{rms} and the "most expected critical" wave groups are finally identified only in terms of the height and period of the central wave. The examined cases of central wave periods were from 6 to 20 seconds with time step 1 second. As far as the maximum central wave heights is concerned, there is no formula analogous to equation (5.10). However, the Gaussian copula presented in Chapter 3, prevents the model itself from generating wave groups with central height above a certain value. This is due to the nature of the inverse error function (see equation (3.16)) which becomes infinite outside the range $[-1,1]$. For this reason, the maximum possible central wave height should be *a priori* calculated for each case of central wave period. This

is a preliminary stage for the application of the deterministic part of the "critical wave groups" method that is not present when regular wave trains are assumed.

In all cases zero initial conditions were assumed at the moment of wave group encounter. This justifies the conceptual idea of the method that ignores what has preceded a wave group event. In other words, any wave effects before the group encounter are included in the selection of the initial conditions. Finally, "critical" wave groups were identified for several roll angle thresholds from 5 to 65 degrees. Examples of transient capsize diagrams for both the regular and irregular "critical wave group" approaches and for angle threshold value 25 degrees are shown in Figure 5.10 and

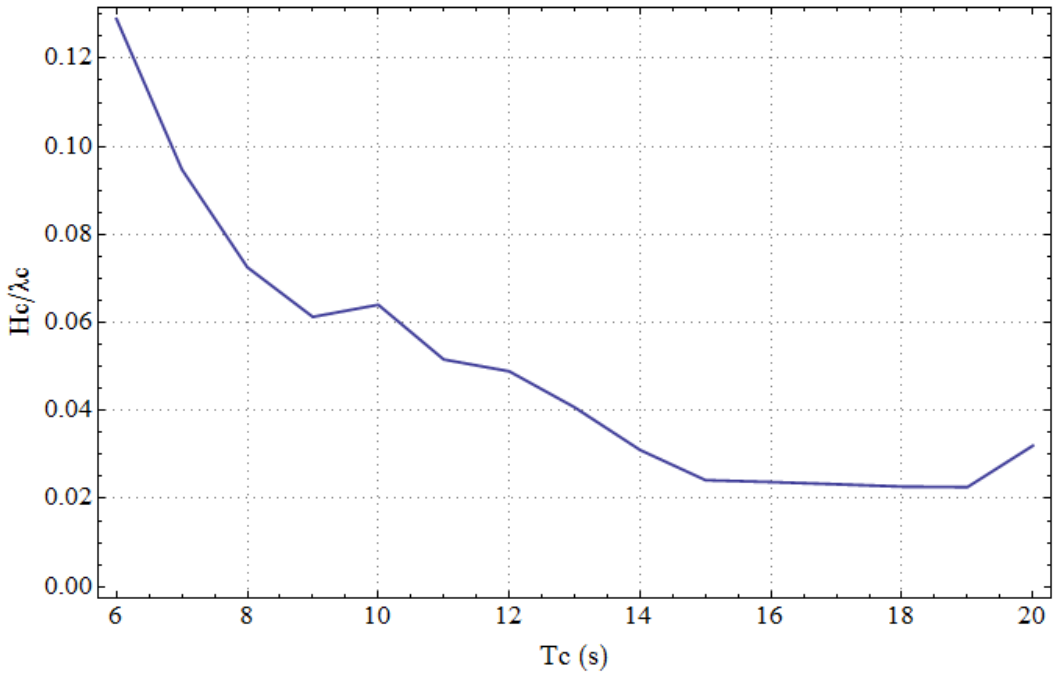

Figure 5.**11**Figure 5.11, respectively. In Figure 5.10, the x axis is the period of the waves and the y axis is the wave steepness, both values being fixed for a regular wave train. In the case of irregular wave groups, however, the diagram is plotted in terms of the characteristics of the central wave. It is noted that in Figure 5.11 the instability area is shifted towards the region of longer waves (Anastopoulos & Spyrou, 2016).

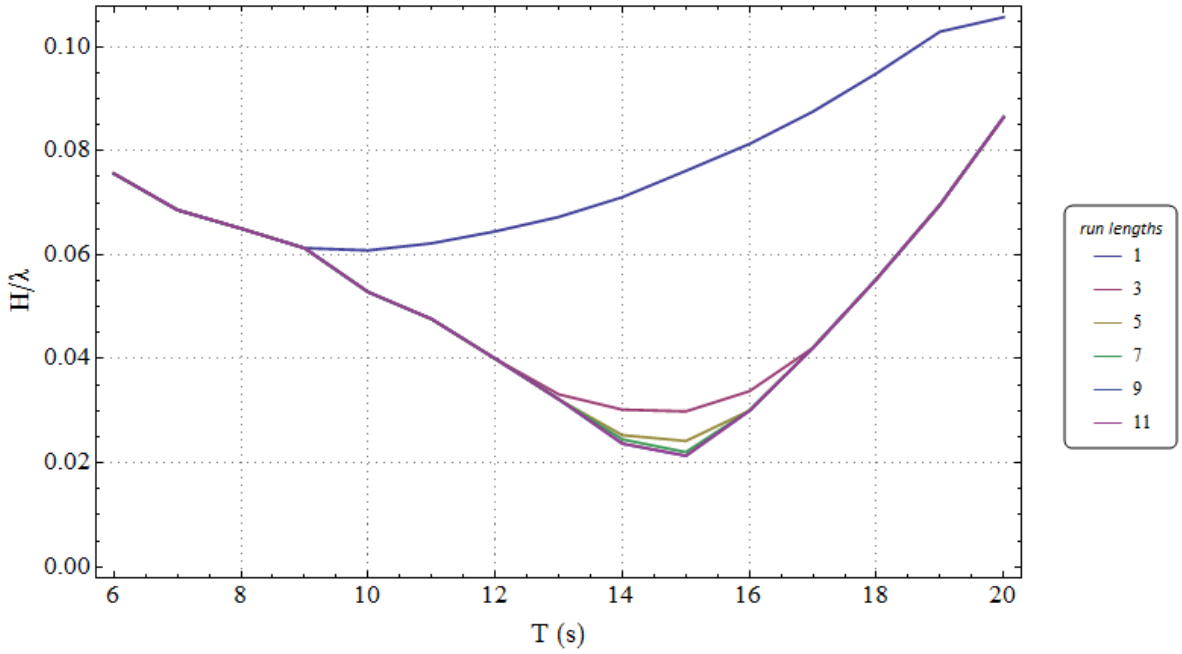

Figure 5.10 Transient capsize diagram for the case of regular wave groups for 25° threshold angle

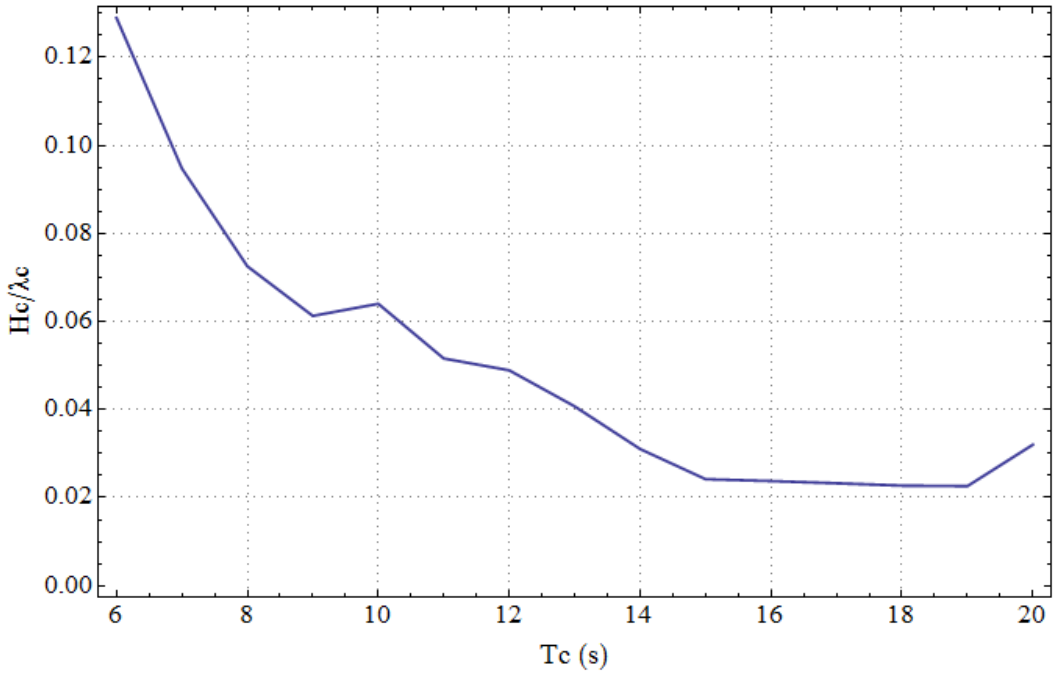

Figure 5.11 Transient capsize diagram for the case of irregular wave groups for 25° threshold angle

Examples of ship response due to regular and irregular wave group excitations are shown in Figure 5.12:

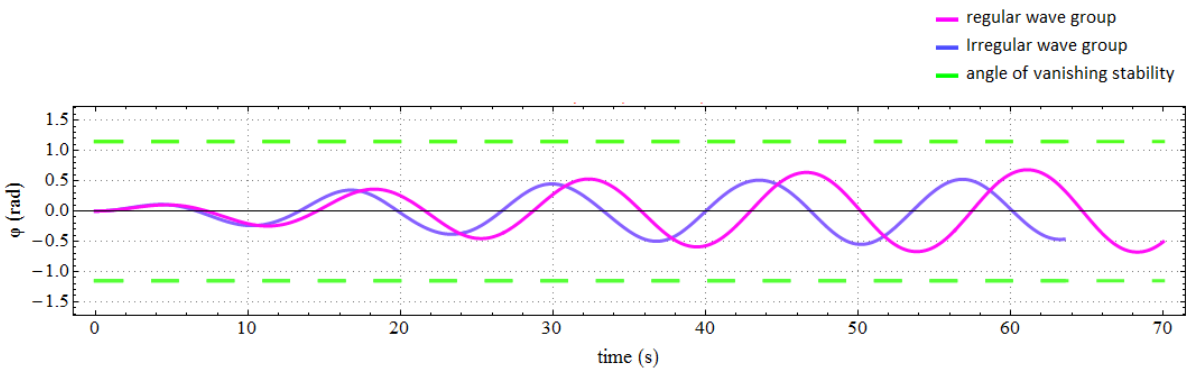

Figure 5.12 Ship's response when it encounters a regular wave group (H=12m, T=14s, run length=5) and an irregular wave group (H_c=12m, T_c=14s, run length=5)

5.4 Probabilistic part

In this final part of the methodology we calculate the probability of encountering any wave group higher than the "critical", determined for a number of different heeling angles. This is used to approximate the probability that the vessel exceeds the specific angle thresholds. To evaluate if the accuracy of the method is improved when considering irregular waveforms, obtained results are tested against direct Monte Carlo simulations of roll motion. Below we describe the procedure for the calculation of the probability of exceedance which differs in the case of irregular wave groups from the one originally proposed by Themelis & Spyrou (2007). It should be noted, however, that in both formulations of the method the number of individual waves constituting a group and, at the same time, participate in the calculation of the probability of exceedance is not essentially equal to the run length. In fact, only the part of the group until the moment of exceedance is considered. For example, for a wave group of j = 5 waves, if exceedance is observed during the 4th wave cycle, only the probability of encountering 4 waves is equal to the probability of instability.

5.4.1 Probability of exceedance – regular case

Let us consider the event $E_{r,n}$ which corresponds to a wave group with:

- n successive waves
- periods T_i that lie within a period range $T_r = [T_{min}, T_{max}]$

- heights that exceed a critical threshold value $H_i \geq H_{cr}$

where $i = 1, \dots, n$. The probability of occurrence of such events derives from the following formula:

$$P[E_{r,n}] = P[H_1, H_2, \dots, H_n \geq H_{cr}, T_1, T_2, \dots, T_n \in T_r] =$$

$$= \int_{T_{min}}^{T_{max}} \int_{H_{cr}}^{\infty} \dots \int_{T_{min}}^{T_{max}} \int_{H_{cr}}^{\infty} f_{H_1,T_1,\dots,H_n,T_n}(h_1, t_1, \dots, h_n, t_n) dh_n dt_n \dots dh_1 dt_1 \quad (5.12)$$

Due to the Markov assumption, equation (5.12) can be simplified (see also equation (3.3)):

$$P[E_{r,n}] = \int_{T_{min}}^{T_{max}} \int_{H_{cr}}^{\infty} \dots \int_{T_{min}}^{T_{max}} \int_{H_{cr}}^{\infty} f_{H_1,T_1}(h_1, t_1)$$

$$\cdot \prod_{i=2}^{n} f_{H_i,T_i|H_{i-1},T_{i-1}}(h_i, t_i | h_{i-1}, t_{i-1}) dh_n dt_n \dots dh_1 dt_1 \quad (5.13)$$

where the conditional probability density functions is calculated according to equation (3.5). The probability density function $f_{H_i,T_i,H_{i-1},T_{i-1}}$ is obtained from the numerical simulations described earlier in this chapter and $f_{H_{i-1},T_{i-1}}$ is derived by integrating $f_{H_i,T_i,H_{i-1},T_{i-1}}$ with respect to the unnecessary random variables H_{i-1} and , T_{i-1}.

The calculation of the total probability of exceedance is achieved by summing up the probabilities of encountering the critical wave events from the different period segments. If we assume that we discretize the periods into l period segments then the total probability of exceedance is calculated by the following formula:

$$P_T = \sum_{r=1}^{l} P_r \quad (5.14)$$

where the probabilities of encountering wave groups that lie in different period segments are treated as mutually exclusive. The probabilities of encountering waves with different run lengths within a period segment are calculated by the following formula:

$$P_r = \sum_{n=1}^{k} P\left[E_{r,n}\right] - \sum_{n=1}^{k-1} \sum_{m=n+1}^{k} P\left[E_{r,n} \cap E_{r,m}\right] + \\ + \sum_{n=1}^{k-2} \sum_{m=n+1}^{k-1} \sum_{q=m+1}^{k} P[E_{r,n} \cap E_{r,m} \cap E_{r,q}] - \cdots + \\ + (-1)^{k-1} P[E_{r,n} \cap E_{r,m} \cap E_{r,q} \ldots \cap E_{r,k}] \qquad (5.15)$$

where k is the maximum run length (here assumed 11) for the r period segment. To illustrate how the intersection of critical wave events is computed let us assume that for a specific period segment T_r we have to calculate the intersection of a critical wave event with run length equal to 1 and height higher than H_{cr1} and a critical wave event with run length equal to 2 and wave heights higher than H_{cr2} (see Figure 5.13). The intersection of these events will be a critical wave event with run length equal to 2, wave height of the first wave higher than H_{cr1} and wave height of the second wave higher than H_{cr2}. By modifying equation (5.12) we obtain:

$$P\left[E_{r,1} \cap E_{r,2}\right] = P[H_1 \geq H_{cr1}, H_2 \geq H_{cr2}, T_1, T_2 \in T_r] = \\ = \int_{T_{min}}^{T_{max}} \int_{H_{cr1}}^{\infty} \int_{T_{min}}^{T_{max}} \int_{H_{cr2}}^{\infty} f_{H_1,T_1.H_2,T_2}(h_1, t_1, h_2, t_2) dh_2 dt_2 dh_1 dt_1 \qquad (5.16)$$

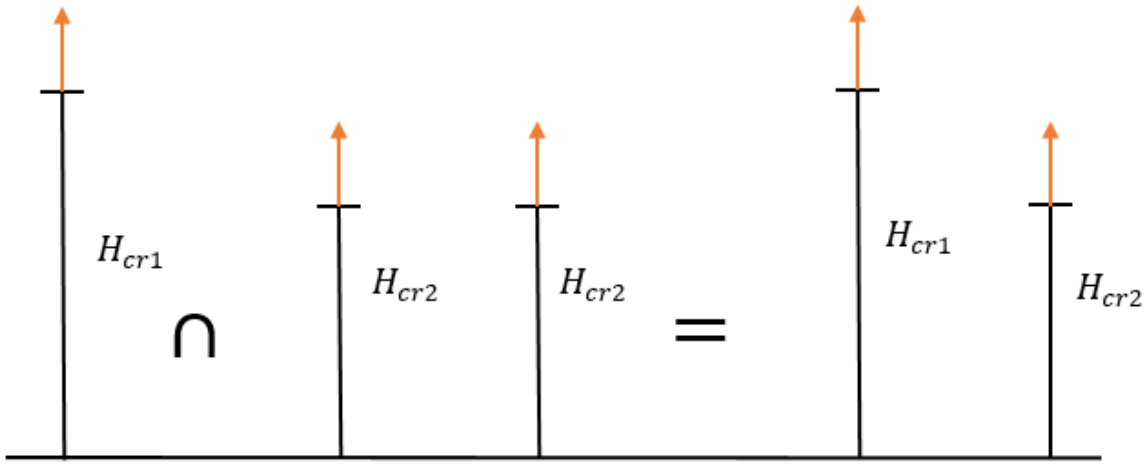

Figure 5.13 Illustration of the intersection of two critical wave events

Finally, the probability of exceedance of the different threshold angles is shown in Figure 5.14. It is noted that the probability was also calculated for the case that the effects of single waves (i.e., run length equal to 1) were neglected. In the same plot we provide the distribution of roll angles derived from Monte Carlo distributions of ship motion.

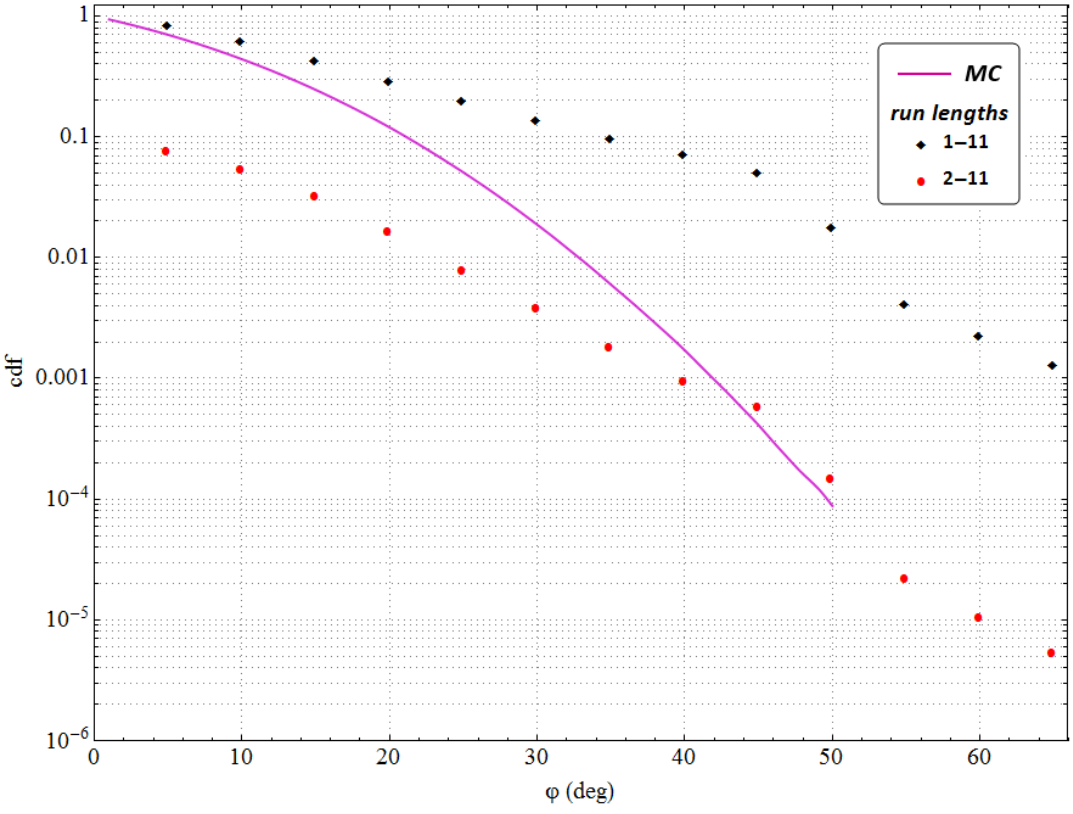

Figure 5.14 Accuracy of the method using regular wave groups

5.4.2 Probability of exceedance – irregular case

In the case of irregular wave groups, the above calculation scheme simplifies since for each central wave period segment there is only one "critical" wave group, the run length of which depends explicitly on the central wave height. Again, "critical" wave group events of different central period segments are treated as mutually exclusive. Thus, the calculation of the total probability of exceedance is computed from equation (5.14).

For a schematic representation of the procedure, see Figure 5.15. As we can see we have a critical wave group with run length of 5 waves. If we assume that the exceedance of the threshold angle is achieved at the time when the central wave passes is encountered (i.e., k = 3), the probability of instability becomes:

$$P_r = P\left[E_{r,3}\right] = \\ = P[H_1 \geq H_{1cr}, H_2 \geq H_{2cr}, H_c \geq H_{3cr}, T_1 \in T_{1r}, T_2 \in T_{2r}, T_3 \in T_{3r}] \quad (5.17)$$

where the calculation of the probabilities in equation (5.17) follows from equation (5.12).

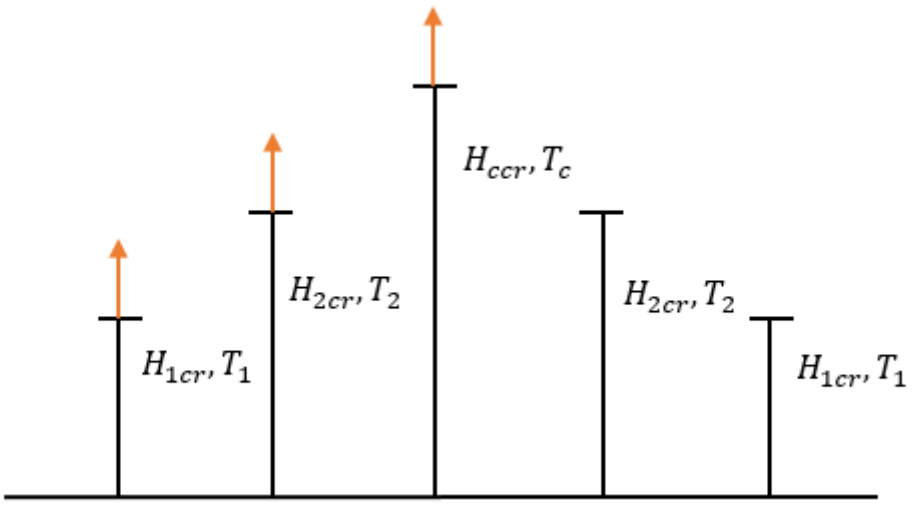

Figure 5.15 Illustration of the calculation of occurrence of critical irregular wave events

Finally, the probability of exceedance of several threshold angles is shown in Figure 5.16. Once again in the same plot we provide the distribution of roll angles derived from Monte Carlo distributions of ship motion.

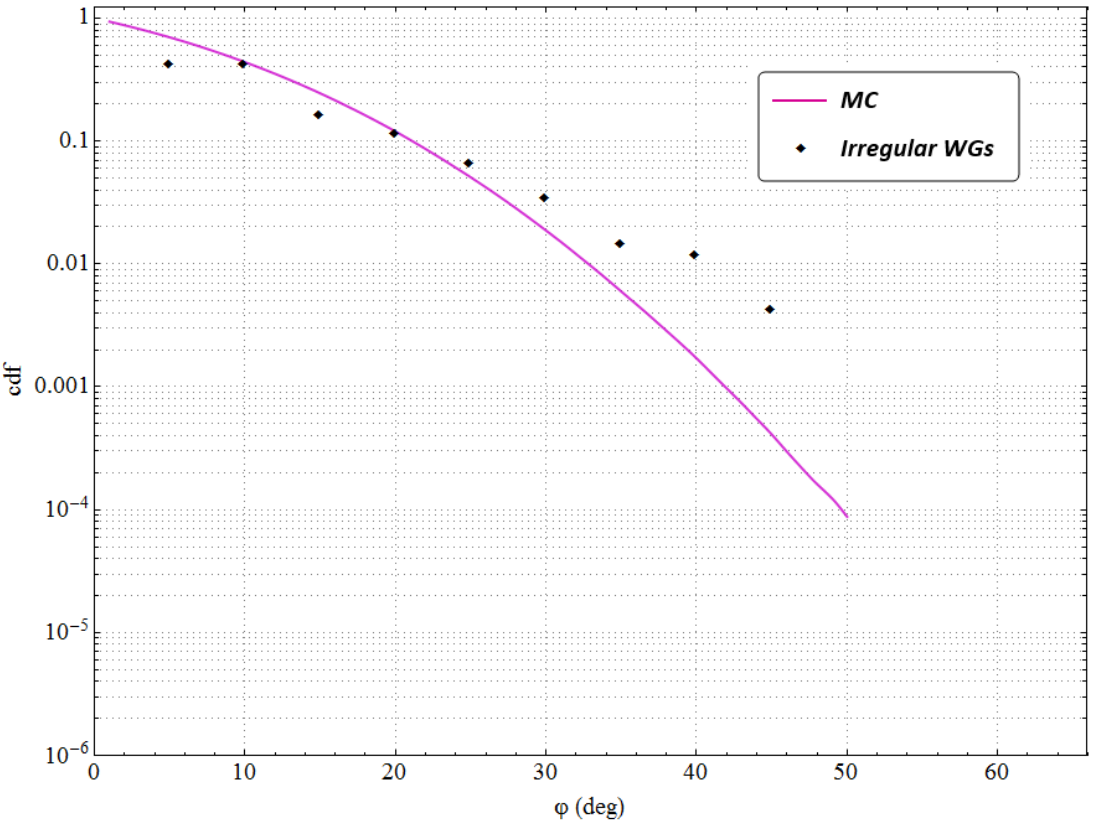

Figure 5.16 Accuracy of the method using irregular wave groups

6. Discussion and final remarks

The estimates for the probability of exceedance derived from the application of the "critical wave groups" method with regular waveforms are inaccurate when single wave events are considered as a degenerated case of wave groups. On the other hand, the accuracy of the method is improved when the effects of single waves are neglected, especially for large heeling angles (40-50 degrees). In such case, the method captures the heavy-tailed structure of the distribution of roll angles. The idea of excluding single-wave groups is reasonable if we consider that in reality is very unlikely that a high wave is not surrounded by other high waves. As realized, the method cannot reflect the physics regarding the relationship between the height of individual waves and the run length. This was an additional motivation for the implementation of the "critical wave groups" method using the model of irregular wave groups developed by Anastopoulos et al. (2016) that relates the height and period of the central wave with the run length.

The accuracy of the "critical wave groups" method with irregular waveforms is very good for heeling angles in the range of 10-35 degrees but diverges for larger values. It should be noted that for heeling angles greater than 45 degrees, the specific calculation scheme fails to produce results. This is because the selection of the Gaussian copula prevents the construction of irregular wave groups with arbitrarily high central wave, as in the case of regular wave groups. In addition, the fact that the employed copula models approximate the distributions produced from the Monte Carlo simulations of the wave field to a certain extent may affect the final results. Furthermore, the accuracy of the method might be improved if the run length is used as a design parameter for the wave groups and does not derive naturally from the selection of the central wave height and period. Nevertheless, more sea states as well as more vessels should be studied before coming to safe conclusions regarding the accuracy of the method.

Overall, the "critical wave groups" method is a promising tool even though many steps can be taken to further improve its accuracy, mostly regarding the deterministic part. The possibility of incorporating a more sophisticated model of roll motion, which accounts for more degrees of freedom, is a significant advantage of the method. As far as the procedure for producing the "most expected" wave groups is concerned, alternative copula models could be employed so that derived distributions agree better with the experimental results. At the same time, the Gaussian copula, that prevents the construction of very high irregular

wave groups, should be replaced. Moreover, the "most expected" wave groups were selected to demonstrate the method and in the future other, less probable, wave group events could be included. Finally, it is also important to assess the effect of the initial conditions of the vessel at the moment of a wave group encounter.

References

Anastopoulos, P.A. (2012). "A probabilistic analysis of ship rolling under the influence of irregular wave groups", Diploma Thesis, National Technical University of Athens, Greece.

Anastopoulos, P.A., Spyrou, K.J., Bassler, C.C. & Belenky, V., (2016). "Towards an improved critical wave groups method for the probabilistic assessment of large ship motions in irregular seas", Probabilistic Engineering Mechanics, 44, pp. 18-27.

Anastopoulos, P.A. & Spyrou, K.J., (2016). "Ship dynamic stability assessment based on realistic wave group excitations", Ocean Engineering, 120, pp. 256-263.

Arhan, M. & Ezraty, R., (1978). "Statistical relations between successive wave heights", Oceanologica Acta, 1(2), pp. 151-158.

Battjes, J.A. & van Vledder, G.P., (1984). "Verification of Kimura's theory for wave group statistics", Proceedings of the 19th International Coastal Engineering Conference, pp. 642–648, ASCE, Houston, TX, USA.

Boccotti, P., (2000). "Wave mechanics for ocean engineering", Elsevier, Oxford, England, ISBN: 978-0-444-50380-0.

Bretschneider, C.L., (1959). "Wave variability and wave spectra for wind generated gravity waves", Tech. Memo. No. 118., Beach Erosion Board, US Army Corps of Eng., Washington, DC.

Cavanié, M., Arhan, M. & Ezraty, R., (1976). "A statistical relationship between individual heights and periods of storm waves", Proceedings of the Conference on the Behavior of Offshore Structures, pp. 354-360, Trondheim, Norway.

Dattatri, J., Raman, H. & Jothishankar, N., (1977). "Wave groups; analysis of run and run length", Proceedings of the 6th Australasian Conference on Hydraulics and Fluid Mechanics, pp. 64-67, Adelaide.

Goda, Y., (1970). "Numerical experiments on wave statistics with spectral simulation", Report, Port and Harbour Research Institute, Vol. 9, No.3, pp. 3-75.

Goda, Y., (1976). "On wave groups", Proceedings of the Conference on the Behavior of Offshore Structures, Vol. 1, pp. 1-14, Trondheim.

Hasselmann, K. et al., (1973). "Measurements of wind-wave growth and swell decay during the Joint North Sea Wave Project (JONSWAP)", Deutschen Hydrographischen Zeitschrift, A.12, pp. 1-95.

Ikeda, Y., Himeno, Y. & Tanaka, N., (1978). "A prediction method for ship roll damping", Report No. 00405 of Department of Naval Architecture, University of Osaka Prefecture.

Kawahara, Y., Maekawa, K., Ikera, Y., (2009). "A simple prediction formula of roll damping of conventional cargo ships on the basis of Ikeda's method and its limitation", Proceedings of the 10th International Conference on Stability of Ships and Ocean Vehicles, St. Petersburg, Russia.

Kim, D.H., Engle, A.H. & Troesch, A.W., (2011). "Estimates of long-term combined wave bending and whipping for two alternative hull forms", SNAME Transactions, 119.

Kim, D.H. & Troesch, A.W., (2013). "Statistical estimation of extreme roll response in short crested irregular head seas", SNAME Transactions, 121.

Kimura, A., (1980). "Statistical properties of random wave groups", 17th International Coastal Engineering Conference, pp. 2955-2973, ASCE, Sydney, Australia.

Longuet-Higgins, M.S., (1952). "On the statistical distribution of the heights of sea waves", Journal of Marine Research, 11(3), pp. 245-66.

Longuet-Higgins, M.S. (1962). "The distribution of intervals between a stationary random function", Philosophical Transactions of the Royal Society of London, Ser. A, 254**,** pp. 557-99.

Longuet-Higgins, M.S., (1975). "On the joint distribution of the periods and amplitudes of sea waves", Journal of Geophysical Research, 80(18), pp. 2688-94.

Longuet-Higgins, M.S., (1983). "On the joint distribution of wave periods and amplitudes in a random wave field", Proceedings of the Royal Society of London A, 389(1797), pp. 241-258.

Longuet-Higgins, M.S., (1984). "Statistical properties of wave groups in a random sea state", Philosophical Transactions of the Royal Society A, 312(1521), pp. 219-250.

Malara, G., Spanos, P.D. & Arena, F., (2014). "Maximum roll angle estimation of a ship in confused sea waves via a quasi-deterministic approach", Elsevier Probabilistic Engineering Mechanics, Vol. 35, pp. 75-81.

Myrhaug, D. & Rue, H., (1998). "Joint distribution of successive wave periods revisited", Journal of Ship Research, 42(3), pp. 199-206.

Næss, A., (1985). "On the distribution of crest to trough wave heights", Ocean Engineering, Elsevier, 12(3), pp. 221–234.

Ochi, M., (1998). "Ocean waves: the stochastic approach", Cambridge University Press, Cambridge, England, ISBN: 978-0-521-01767-1.

Patton, A.J., (2006). "Modelling asymmetric exchange rate dependence", International Economic Review, 47(2), pp. 527-556.

Rodriguez, G.R. & Guedes Soares, C., (2001). "Correlation between successive wave heights and periods in mixed sea states", Ocean Engineering, 28(8): pp. 1009-1030.

Rye, H., (1974). "Wave group formation among storm waves", Proceedings of the 14th International Conference on Coastal Engineering, pp. 164 – 183, Copenhagen, Denmark.

Schweizer, B. & Wolff, E., (1981). "On nonparametric measures of dependence for random variables", Annals of Statistics, 9(4), pp. 879-885.

Sclavounos, P.D., (2012). "Karhunen-Loève representation of stochastic ocean waves", Proceedings of the Royal Society A, 468(2145), pp. 2574-2594.

Sklar, A., (1959). "Fonctions de répartition à n dimensions et leurs marges", Annales de l' I.S.U.P., Publ. Inst. Statist. Univ. Paris, 8.

Slepian, D. & Pollack, H.O., (1961). "Prolate spheroidal wave functions, Fourier analysis and uncertainty – I", Bell System Technical Journal 40(1), pp. 43-63.

Spyrou, K.J., (2014). "Ευστάθεια διατοιχισμού πλοίου και υπόβαθρο κανονισμών", Course notes, National Technical University of Athens, Greece.

Stansell, P., Wolfram, J. & Linfoot, B., (2002). "Statistics of wave groups measured in the northern North Sea: Comparisons between time series and spectral predictions", Applied Ocean Research, Elsevier, 24(2), pp. 91-106.

Stansell, P., Wolfram, J. & Linfoot, B., (2004). "Improved joint probability distribution for ocean wave heights and periods", Journal of Fluid Mechanics, 503, pp. 273-297.

Tayfun, M., (1990). "Distribution of large wave heights", Journal of Waterway, Port, Coastal and Ocean Engineering, 116(6), pp. 686–707.

Themelis, N., (2008). "Probabilistic assessment of ship dynamic stability in waves", Doctoral Thesis, National Technical University of Athens, Greece.

Themelis, N. & Spyrou, K.J., (2007). "Probabilistic assessment of ship stability", SNAME Transactions, 115, pp. 181-206.

van Vledder, G.P., (1992). "Statistics of wave group parameters", Proceedings of the 23rd International Coastal Engineering Conference, Vol. 1, pp. 946–959, ASCE, New York, NY, USA.

Wilson, J. & Baird, W.F., (1972). "A discussion of some measured wave data", Proceedings of the 13th International Coastal Engineering Conference, pp. 113-130, ASCE, Vancouver, Canada.